Exactly solvable single-channel and multichannel models (lessons in quantum intuition)

B. N. Zakhar'ev, N. A. Kostov, and E. B. Plekhanov

Joint Institute for Nuclear Research, Dubna

Fiz. Elem. Chastits At. Yadra **21**, 914–962 (July–August 1990)

It is only in the most recent years, after more than half a century of development of quantum mechanics, that there have begun to appear "pictures" which demonstrate the response of potentials to variations of individual spectral parameters (energy levels, reduced widths of states, etc.) for single-channel and multichannel exactly solvable models. The most instructive illustrations are given in this review. Also considered are: 1) the unexpected and intriguing behavior of wave packets in the below-barrier regions, recognition of which can deepen understanding of the time evolution of tunneling; 2) separation of the motion of waves from channel to channel or with respect to periods of an external field (with respect to a discrete variable that labels the channels or periods), which casts new light on multichannel processes and on the concept of a quasimomentum and quasienergy for a particle in a periodic field.

INTRODUCTION

Quantum mechanics has already celebrated its half-century jubilee, but the intensity of its development does not flag. If we restrict ourselves to the nucleon level of the structure of matter (and do not penetrate into its quark details), a large proportion of the phenomena around us is amenable to a nonrelativistic description. Thus, the prospects for the development of the quantum-mechanical approach are practically unlimited. In particular, this applies to the multiparticle and associated multichannel aspects of the theory. That which has already been elucidated is but a drop in the ocean of what is as yet uncomprehended, although the behavior already revealed has led to fantastic applied results.

The avalanche-like accumulation of information in the field of quantum physics calls for new forms to assimilate it. An example of the response to this requirement is the book by Brand and Dahmen: The Picturebook of Quantum Mechanics.[54] Many other instructive illustrations of quantum behavior can be proposed (one of the authors of the present paper himself intended even earlier to write such a book, admittedly with other pictures). Acquaintance with new examples of this kind is an effective way of developing our physical intuition.

In recent years there have appeared a number of studies with explicit solutions of quantum problems that enable one to clarify the connection between the interaction parameters of the particles and the spectral properties and wave functions of the corresponding systems (in particular, the scattering data).

We have collected together in this review the most striking results from these publications, augmenting them with perspicuous illustrations and new explanatory commentaries. Maximal accessibility of the presentation must facilitate their use in scientific and applied purposes. It is remarkable that only now (50 years after the creation of quantum mechanics) has use been made of the remarkable possibility of the inverse-problem approach to demonstrate directly how the potentials are rearranged when there is a shift of, for example, the positions of individual levels or variation of the values of their reduced widths. We have become the possessors of simple algorithms for constructing quantum systems with desired spectral properties (the analogy with a child constructor suggests itself). The pedagogical value of this information calls for its most rapid introduction into courses on quantum mechanics.

In Sec. 1 we consider one-dimensional, single-channel problems, in particular new aspects of the "old" but very important quantum effect of below-barrier tunneling (resonance transparency of a system of barriers and time evolution of the below-barrier motion). Section 2 is devoted to multichannel systems, to which the solution of multidimensional and multiparticle problems reduces. We here discuss some as yet insufficiently understood mechanisms of occurrence of scattering resonances (standing waves with respect to a discrete variable that labels the channels and bound states in the continuum—above-barrier trapping of waves). We also discuss a new view of the motion of waves in a periodic field, which casts light on the meaning of the concepts of quasimomentum and quasienergy, namely, they are the ordinary momentum and energy of free motion with respect to a discrete variable that labels the periods (the picture of the motion in a periodic field becomes simpler if one separates the oscillations within one period—ordinary standing waves—from waves that travel through the lattice of periods.) Section 3 contains commentaries on the literature; in particular, we briefly consider the directions of intense study which are leading, in our opinion, to the creation of a unified theory of exactly solvable models (see Refs. 10, 24, 38, and 42).

1. ONE-DIMENSIONAL AND SINGLE-CHANNEL MODELS

Deformations of the potential when the spectral parameters are varied

In this section we present graphs that illustrate the influence of individual spectral parameters (positions of levels or of the R-matrix resonances plus normalization constants or reduced widths) on the form of the potential. We obtained many of these graphs specially for the review. We do not give here the formulas of the inverse problem for the potentials and wave functions (see the more general case in Sec. 2) in order to concentrate attention on the qualitative aspects of the connection $V(x) \leftrightarrow$spectrum.

The approach of the inverse problem is remarkable in that it enables one to consider from the other side the connec-

 0090-4759/90/040384-23$04.00

tion between the forces and the physical properties of systems in which they act. It becomes possible to construct systems with required properties, provided that one does not go beyond the framework of the admissible spectral parameters and scattering data.

We take an infinite rectangular potential well with width a and see how it is deformed when we change its spectral properties: the energy levels E_λ and normalization constants. As the latter, we can take the numbers γ_λ, which are the values of the derivatives of the normalized wave functions at the right wall ($x = a$) of the potential well:

$$\gamma_\lambda \equiv \Psi'_\lambda(x=a); \quad \int_0^a |\Psi_\lambda(x)|^2 dx = 1. \tag{1}$$

These numbers γ_λ are the amplitudes of the reduced widths of the states with energy E_λ and are important spectral parameters. We should mention that the reduced widths can also be given other definitions (see, for example, Ref. 20, p. 14).

The set $\{E_\lambda, \gamma_\lambda\}$ completely determines the shape of the potential. In our case the original potential is $V(0 \leqslant x \leqslant a) = \text{const} = 0$. The following series of figures (we have taken many of them from Ref. 83) demonstrates the response of the shape of the potential to variation of some of these parameters (Fig. 1, Refs. 83 and 88).

In the infinite set $\{E_\lambda, \gamma_\lambda\}$ we shall initially vary only the one normalization γ_1 of the ground state, requiring $\Psi_1(x)$ to decrease more steeply in modulus at the wall $x = a$. Several such eigenfunctions are shown in Fig. 1b. For the corresponding potentials, see Fig. 1a. One can understand qualitatively why the shape of the potential reacts in such a manner to an increase in the steepness of the function $\Psi_1(x)$ at $x = a$. If the potential did not change, the increase of $\Psi_1(x)$ would reduce to multiplication of the function by a number, and this would violate the normalization $\int_0^a |\Psi_\lambda(x)|^2 dx = 1$. This enhanced growth of Ψ_1 with increasing distance from $x = a$ must be compensated by an earlier transition to decrease if the integral of the square of the wave function of the ground state is to remain normalized to unity. It is precisely the deepening of the potential near $x = a$ that ensures such behavior of $\Psi_1(x)$ (the deeper the bottom of the potential below a given level, the higher the local frequency of oscillations of the corresponding eigenfunction). But subsequently it is necessary to force the function, which must not change sign—nodes of the ground state

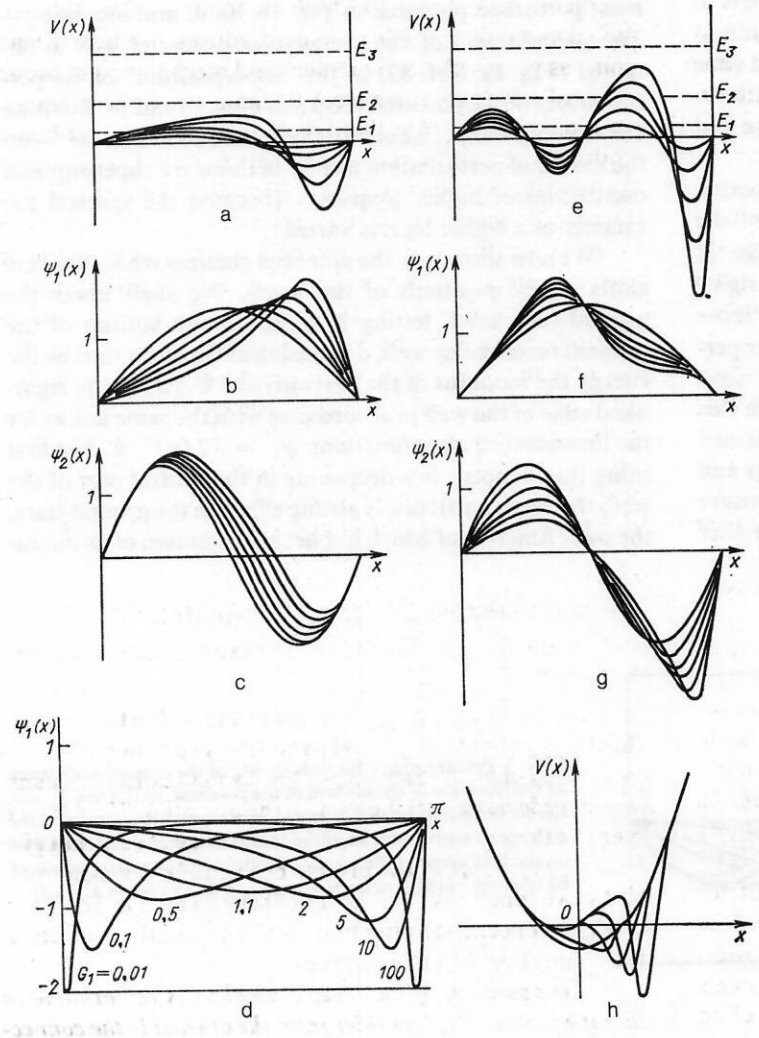

FIG. 1. Change in the shape of the potential (a,e,h) and wave functions $\Psi_\lambda(x)$ (b,c,d,f,g) as the result of variation of γ_λ, the values of the derivatives Ψ'_λ at the wall of an infinite well (a–e) or at its center (h) (Refs. 83 and 88): a) deformation of the bottom of an infinite rectangular well as a result of an increase in the slope $|\gamma_1|$ of the ground-state wave function Ψ_1 at the righthand wall; all the levels E_λ and the derivatives $\gamma_{\lambda \neq 1}$ remain unchanged; b) ground-state wave functions Ψ_1 corresponding to the potentials in Fig. 1a; c) wave functions $\Psi_2(x)$ of the first excited states in the potentials shown in Fig. 1a; d) the change in Ψ_1 due to a decrease and an increase of the reduced width (our calculation), $\gamma_1 = (2/\pi)^{1/2} G_1 / k_1$; e) deformation of the potential as a result of a change of the derivative γ_2 of the eigenfunction Ψ_2 at the righthand edge of the well (the energy levels E_λ and $\gamma_{\lambda \neq 2}$ are not changed); f) ground-state wave functions corresponding to the potentials in Fig. 1e; g) wave functions Ψ_1 of the first excited states that correspond to the potentials in Fig. 1e; h) deformation of the oscillator well as a result of a change of the derivative of the ground-state wave function at the point $x = 0$.

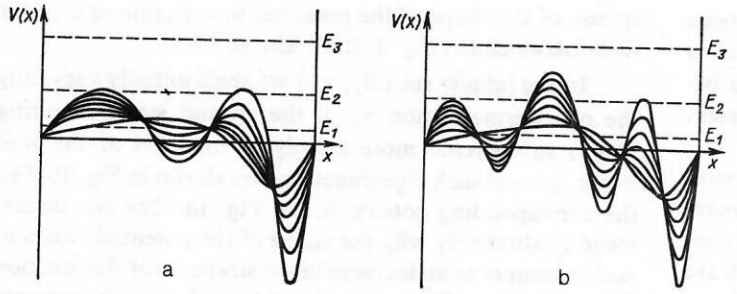

FIG. 2. Deformation of an infinite rectangular potential well as a result of simultaneous changes in several parameters γ_λ (γ_1 and γ_2 in Fig. 1a, and γ_1 and γ_3 in Fig. 1b; Ref. 83): a) γ_1 is equal to the value that corresponds to the maximal deformation of the well in Fig. 1a, and γ_2 is increased; b) γ_1 is fixed as for the potential with maximal deformation in Fig. 1a, and γ_3 is increased.

are forbidden—to sink to zero at the point $x = a$. This is achieved by the repulsive part of the correction to the original potential in the left-hand part of the well—below the barrier the function is appreciably smaller than the unperturbed function. At the same time, the repulsive and attractive parts of the perturbation of the potential mutually compensate their influence on the energy levels; namely, in the well with distorted bottom they all remain the same as in the infinite rectangular well. The wave functions of the excited states adjust to the new shape of the potential, but in such a way that the values of $\Psi'_\lambda(a)$ remain unchanged; see Fig. 1c, which shows the second eigenfunction for different values of the parameter γ_1 (at the right-hand edge, the functions merge into a single curve). If instead of increasing γ_1 in modulus we decrease it, we must expect the opposite reaction of the perturbing potential—instead of attraction near a there will be repulsion and vice versa in the left-hand part of the well. In the wave function the maximum (in modulus) will be shifted to the right, and not to the left. Figure 1d (our calculation) shows the gradual change, symmetric with respect to the center of the well, of $\Psi_1(x)$ with decrease and increase of γ_1.

We now consider how the potential and wave function react to variation of the normalization constant γ_2 of the second state (see Figs. 1e–1g, Ref. 83). As in the case of variation of γ_1, the potential becomes deeper at the right-hand edge of the well with increasing γ_2 (Fig. 1e), but more rapidly than in Fig. 1a. This happens because a stronger perturbation of the potential is required to deform the wave function of a state with higher energy. To compensate this strong attraction, a higher repulsive barrier, which is formed to the left of the deepening, is required. A small dip and barrier are needed in the left-hand half of the well to ensure that the function $\Psi_1(x)$ (Fig. 1f), which has become smaller in the right-hand half of the well, can increase in the left-hand part of it in order to preserve the normalization and terminate the oscillation at the left wall with zero value [and for some reason with unchanged slope; it is also not clear why the functions $\Psi_1(x)$ and $\Psi_2(x)$ pass through a common point at the center of the well for all values].

It is interesting to compare the series of spectrally equivalent potentials for the infinite rectangular well (in Fig. 1a) with an analogous series for an oscillator (Fig. 1h, Ref. 88). The analogy cannot be complete; in the second case the derivative of the eigenfunction is changed, not at the well edge, but at its center (the derivative can also be regarded as a normalization constant). Figures for deformations of the Coulomb interaction that do not distort the spectrum are given in Ref. 62.

We now take for γ_1 the value that corresponds to the most perturbed potential in Fig. 1a, fix it, and increase γ_2. The perturbation of the rectangular potential well is obtained (Fig. 2a, Ref. 83) as the "superposition" of the perturbations of the potential shown in Figs. 1a and 1e. But if we vary, not γ_2, but γ_3, we obtain the potentials in Fig. 2b[83]—on the maximal perturbation in Fig. 1a there are superimposed oscillations of higher frequency (because the spectral parameter of a higher level is varied).

We now show how the potential changes when there are shifts in the positions of the levels. We shall lower the ground-state level, letting it approach the bottom of the original rectangular well, decreasing at the same time as the energy the modulus of the derivative of $\Psi_1(x)$ at the right-hand edge of the well in accordance with the same law as for the unperturbed eigenfunctions: $\gamma_1 = (2/\pi)^{1/2}k$. The first thing that happens is a deepening in the central part of the well; this has a particularly strong effect on the ground state, the wave function of which has here a maximum of its modu-

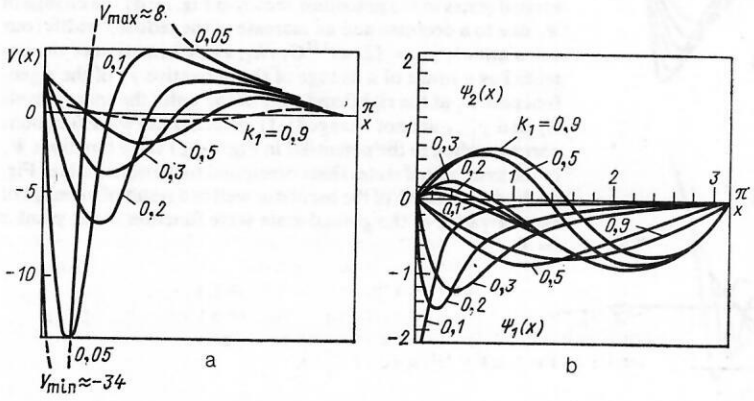

FIG. 3. Perturbations due to lowering of the ground-state level: a) deformation of the bottom of the potential well when $E_1 \to 0$; the deepening of the well draws E_1 downward; the barrier on the right decreases γ_1 and simultaneously, together with the barrier on the left, keeps all the excited levels in the previous positions; b) changes of the functions $\Psi_1(x)$ and $\Psi_2(x)$ when $E_1 \to 0$.

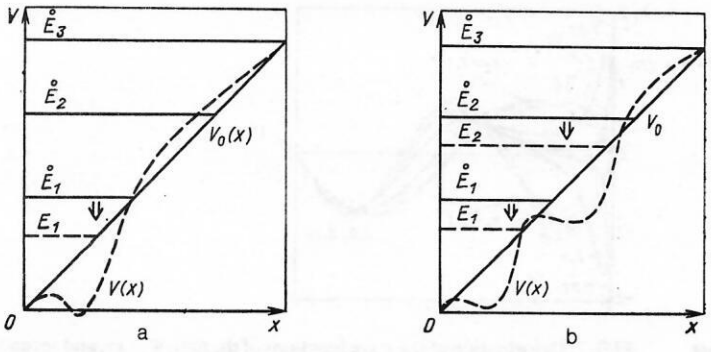

FIG. 4. Shift of levels in a linear potential well: a) shift of one level E_1; b) shift of two levels E_1 and E_2. The broken curve is the distortion of the potential needed for this.

lus (see Fig. 3). Repulsive barriers at the edges of the well have a weaker influence on E_1, since there $\Psi_1(x)$ is small. With further lowering of E_1, the deepening becomes more pronounced, while the decrease of γ_1 increases the right-hand barrier, shifting to the left the deepening, which drags the maximum of $\Psi_1(x)$ after it. The excited levels remain in the previous positions, because the repulsion of the perturbation compensates the action of the attraction on them. Similar arguments also explain the deformation of a linear infinite well (Fig. 4, Ref. 67) when one or two levels are lowered. Judging from Fig. 4, the shift of the ever higher levels E_λ in wells with nonvertical walls occurs because of localized deformations of the wall—"icicles," which move ever higher in energy and further from the origin with increasing λ (perturbations damped with λ in the region in which the lowest states are concentrated).

When the first level is raised to the second with $\gamma_1 = (2/\pi)^{1/2}k_1 \to \gamma_2$, the ground-state function becomes more and more similar in the right-hand part of the well to the function $\Psi_2(x)$ (Fig. 5a). Indeed, in the limit $E_1 \to E_2$ the two functions are solutions of the same equation with almost identical boundary conditions and almost equal energies. In the region of the node of the function $\Psi_2(x)$, the barrier almost identical boundary conditions and almost equal energies. In the region of the node of the function $\Psi_2(x)$, the barrier of the perturbing potential (Fig. 5b) makes $\Psi_1(x)$ small too, while to the left of this node the two functions differ approximately only in sign. It can be seen from Figs. 3a and 5b that small shifts of E_1 downward and upward correspond to perturbations of $V(x)$ that differ mainly in the sign.

A similar picture is observed on the lowering $E_2 \to E_1$, $\gamma_2 \to \gamma_1$ (Fig. 6) and on the approach $E_2 \to E_3$, $\gamma_2 \to \gamma_3$ (Fig. 7) or $E_3 \to E_2$, $\gamma_3 \to \gamma_2$ (Fig. 8).

If one specifies a derivative γ_ν of one of the approaching states that differs strongly from the derivative $\gamma_{\nu\pm1}$ of the other, the functions $\Psi_\nu(x)$ and $\Psi_{\nu\pm1}$ (Fig. 9) of the two states are nevertheless approximately equal except for constant factors (which may be different to the left and to the right of the nodes in order to compensate the difference of the normalization integrals; violation of constancy of the ratio $\Psi_\nu/\Psi_{\nu\pm1}$ occurs only below the barrier, where both functions are small.

We note, in passing, a helpful *rule of behavior of the wave function in the below-barrier region. In it, the function cannot have more than one node, and also the function does not have positive maxima and negative minima.*[1)]

One may be concerned about whether the perturbing potentials turn out to be symmetric.[2)] Figure 10a (Ref. 83) shows the deformation of the bottom of the potential well when the ground-state level is raised to the first excited level. One can see the formation at the walls of two symmetric deepenings, separated by an increasing central barrier. The barrier in the center pushes the ground state upwards more strongly than the first excited state, since here $\Psi_1(x)$ is larger in modulus than $\Psi_2(x)$, which has here a node. Conversely, the wells at the edges draw down more strongly the excited state with two separated maxima of the modulus $|\Psi_2(x)|$ than they do the ground state, for which $\Psi_1(x)$ is smaller in modulus at the edges. Thus, under the influence of the perturbations shown in Fig. 10a the second level must remain in its position, since the influence of the attraction and the in-

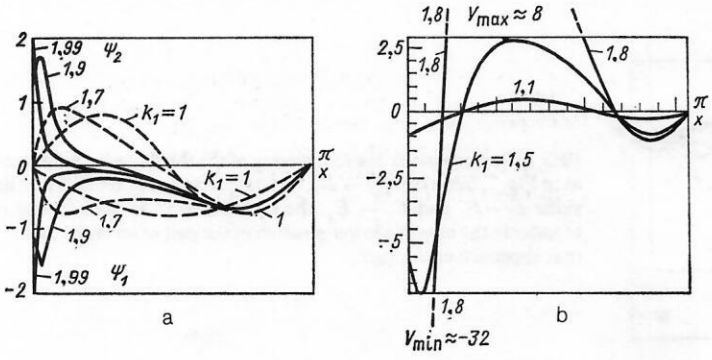

FIG. 5. Perturbations due to the shift $E_1 \to E_2$: a) approach in modulus of the wave functions of the ground state, $\Psi_1(x)$, and of the first excited state, $\Psi_2(x)$, when the level E_1 is raised to E_2; to the right of the node of $\Psi_2(x)$, functions Ψ_1 with $k > 1.9$ become approximately equal to Ψ_2, while on the left they differ almost only in the sign; the change of sign takes place in the below-barrier region); b) the barrier of the perturbing potential in the center of the well pushes E_1 upward; the deepening on the right increases $|\gamma_1|$ and simultaneously, together with the left-hand deepening, compensates the influence of the central barrier on the excited levels (cf. Fig. 3).

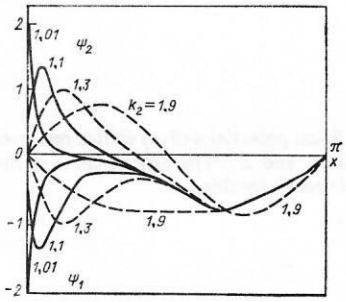

FIG. 6. A picture like that shown in Fig. 5a, the only difference being that the approach of the two lowest levels occurs because E_2 is lowered to E_1.

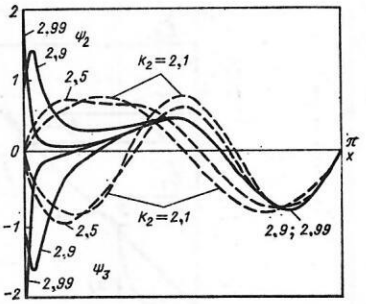

FIG. 7. Deformation of the wave functions of the first, $\Psi_2(x)$, and second, $\Psi_1(x)$, excited states as a result of the raising $E_2 \to E_3$.

fluence of the repulsion compensate each other. Figure 10b (Ref. 83) shows how the ground-state wave function changes at the same time—it gradually splits into two states in the separate wells. As the levels approach, $|\Psi_1(x)|$ in the center decreases together with the necessity for repulsion at this position (a level is more effectively influenced where the probability is greater) (see the slight minimum at the center of the barrier in Fig. 10a; the same thing happens in an oscillator; see Fig. 11e).

Note also that the shape of the symmetric (with respect to the center) potential, as in Figs. 10a and 10b (Ref. 83) and 11a–11e (Ref. 83), is completely determined by its energy levels, and the normalization constants γ_i are also specified by the set of eigenvalues (see Ref. 20, pp. 40–43). Therefore, together with the shift of the level the normalization γ_1 changes, as can be seen in Fig. 10b (Ref. 83) (the normalizations are adjusted to the given levels).

A further illustration of the doubling of a symmetric potential well when the two lowest levels approach each other is provided by Fig. 11, which shows a series of potentials obtained from the oscillator potential with the perturbing corrections that are required to raise the first level to the second, and by Fig. 12 (Ref. 75) for transparent (reflectionless, "two-soliton") potentials ($E_1 \to \leftarrow E_2$).

If one does not make the first level approach the second, but rather makes the second approach the third, then we find that in the potential of the perturbation (see Fig. 13, Ref. 83) there are now two repulsive maxima at the positions at which $|\Psi_2(x)|$ has maxima. But the three wells near the three maxima of $|\Psi_3(x)|$ do not raise E_3 (they keep this level at its previous position). When they act on the relatively slowly varying ground state, the oscillations of the perturbation potential also compensate each other. The higher states mainly feel only the mean value $\int V(x)\Psi_\lambda^2(x)dx$ of the perturbation, which in our case is near zero.

Having understood qualitatively how the potential must change when one spectral parameter is varied, it is easier to analyze the more complicated case of the approach of three levels in the transparent potential in Fig. 14 (Ref. 75). The raising of the bottom of the well at its center pushes upward the ground state and has less effect on the second level (node of Ψ_2). The three dips in the bottom of the well are formed to act on the three maxima of $|\Psi_3(x)|$, in order to lower E_3, which is also assisted by broadening of the upper part of the well. Note that the wave function of the second level tends to zero in the central well. The reason for this is that $\Psi_1(x)$, $\Psi_2(x)$, and $\Psi_3(x)$, being solutions of the same equation for nearly equal energies, must behave similarly apart from a "constant" factor. The violation of this requirement can be reduced to a minimum for functions with different numbers of nodes by making the functions tend to zero in the region of the nodes (all three in the below-barrier regions, and the second one in the central zone of attraction).

A new example of "superposition" of perturbations is shown in Fig. 15 (Ref. 83). We first shift E_1 to E_2 and obtain one of the series of potentials of Fig. 10a—it can also readily be found in Fig. 15. Now, for the shifted E_1, fixed in the new position, we move E_2 upward. We can expect that then the perturbations represented in Fig. 13a will be superimposed on one of the potentials in Fig. 10a. We do indeed see these "sums" of perturbations in Fig. 15. If we now fix certain of these upward shifts of the two lowest levels and begin to

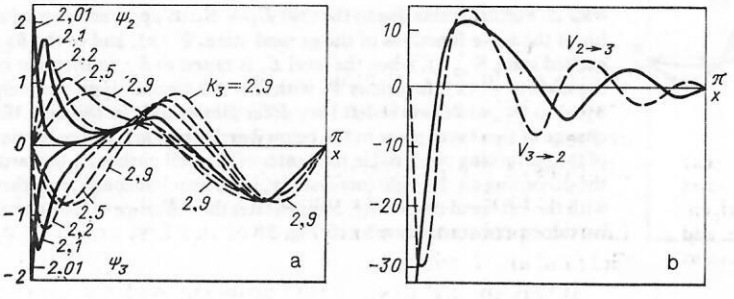

FIG. 8. Perturbations due to lowering of the third level: a) the same as in Fig. 7, but when $E_3 \to E_2$; b) comparison of potentials for the shifts $E_3 \to E_2$ and $E_2 \to E_3$; the potential well at the left wall is broader in the case of a lower position of the pair of levels E_2 and E_3 that approach each other.

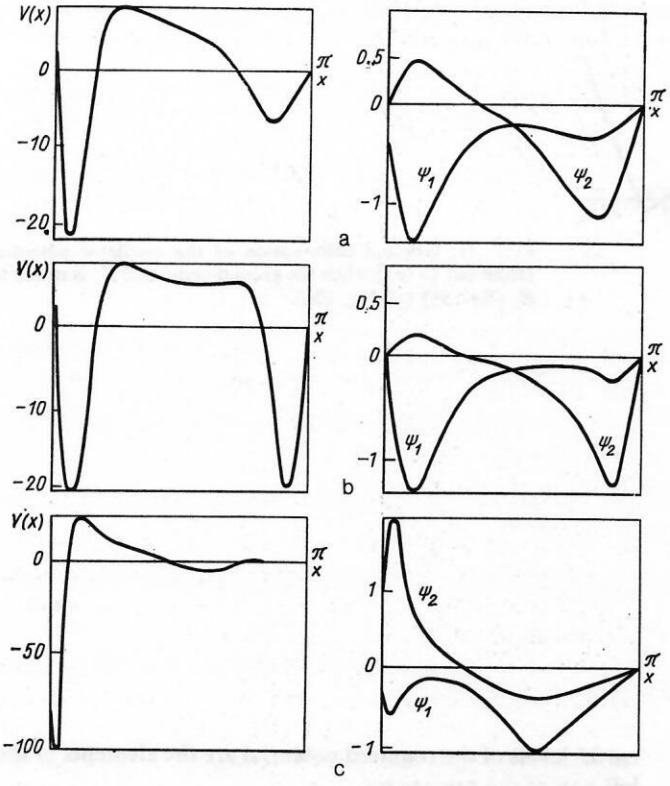

FIG. 9. Potentials of the perturbation and the functions Ψ_1 and Ψ_2 for level E_2 lowered to E_1 ($k_2 = 1.2$): a) $\gamma_2 = 3(2/\pi)^{1/2}/k_2$; b) $\nu_2 = 6(2/\pi)^{1/2}/k_2$; c) $\nu_2 = 0.3(2/\pi)^{1/2}/k_2$.

move the third upward, then on the potential in the series of Fig. 15 there is superimposed an elementary perturbation with three maxima, as is shown in Fig. 16 (Ref. 83).

It is interesting to see how the $V(x) \leftarrow$ spectrum connection is influenced by the rate of ascent of the potential walls for different types of wells: with infinite vertical walls (Figs. 1–3), with walls that rise linearly (Fig. 4) and as the square of the distance (Fig. 11), and for potentials that vanish at large distances (Figs. 12 and 14). One can trace the common features and differences in the behavior of the shape of the potentials and the functions when the spectral parameters are perturbed.

Hitherto, we have restricted ourselves to shifts of levels in the interval between their neighbors. But displacement of a level beyond the neighbors (for example, a shift of E_1 into the interval between the second and third levels, $E_2 < E'_1 < E_3$) is equivalent to a succession of the restricted displacements (E_1 to the position of E_2; E_2 to the position of E'_1; see Fig. 17).

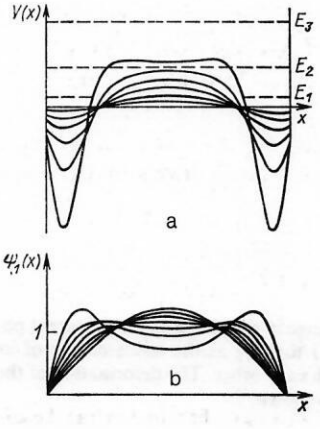

FIG. 10. Approach of levels with the symmetry of $V(x)$ and $|\Psi_\nu|(x)$ maintained: a) deformation of the potential when the ground-state level E_1 is raised to the first excited level (cf. Fig. 11); b) change in the eigenfunction Ψ_1 when $E_1 \rightarrow E_2$; the coupling between the eigenvalues and normalization constants in a symmetric well leads to a simultaneous change of the derivatives at $x = a$ (cf. Figs. 11 and 12).

Recovery of the potential from spectral parameters

The R-matrix approach

We shall show how, following the idea of the "quantum constructor," one can approximately solve the inverse problem: "construct" a system with given spectral set $\{E_\nu, \gamma_\nu\}$ for unknown potential $V(r)$ by successively correcting the spectral data $\{E_\mu, \gamma_\mu\}$ of the auxiliary problem with potential V_0 [by shifting to the necessary positions E_ν the lower levels E_μ of the original auxiliary potential $V_0(r)$ and correcting, accordingly, the reduced widths $\gamma \rightarrow \gamma_\nu$]. This is, moreover, the first example of numerical recovery of the shape of the potential from the spectral data in the approach of the R-matrix theory of scattering by means of analytic solutions of Bargmann type.[52]

The formalism of the one-dimensional inverse Sturm–Liouville problem on a finite interval was first proposed by Gel'fand and Levitan.[8]

It was applied to scattering problems with finite-range

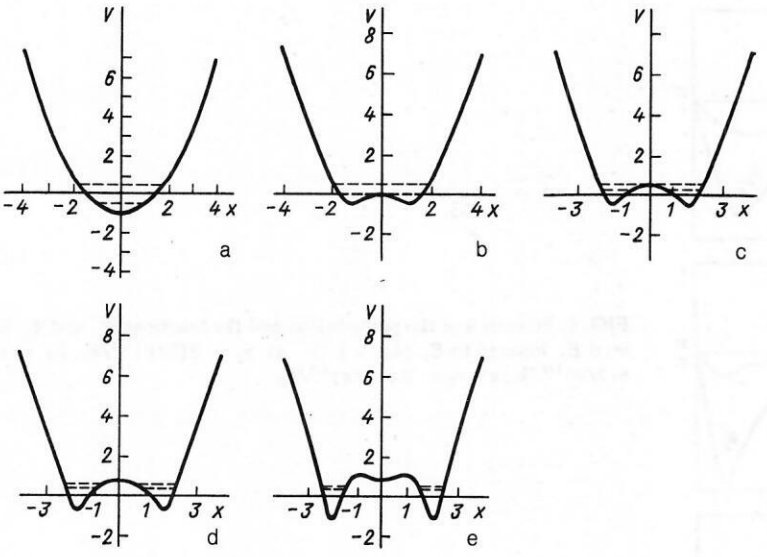

FIG. 11. Gradual deformation of the oscillator potential [from (a) to (e)] when the ground-statel evel E_1 is raised to E_2 (Ref. 88) (cf. Fig. 10a).

potentials (R-matrix theory) in Ref. 14. In Ref. 55 there is a discussion of the use of the R matrix as original information in the inverse problem, though admittedly in the less convenient (in the given case) formalism on a half-axis ($0 \leqslant r < \infty$). See Refs. 20 and 52 for the multichannel generalization of the R-matrix inverse problem and various exactly solvable models for finite-range interaction.

The formalism that we shall use here is a special single-channel case of the general theory of the multichannel inverse problem[52] presented in the second part of the review.

The R-matrix Bargmann wave functions constructed from the M pairs $\{E_\nu,\gamma_\nu\}$ of spectral parameters of the lowest M levels of the required potential are the elements of the left half of the row vector

$$\Psi_0^T(r) = \Psi_0^T(r)\,\hat{P}^{-1}(r) \qquad (2)$$

with elements $\{\Psi(E_\nu,r),\ldots,\Psi(E_\mu,r)\ldots\}$, where ν and μ take the values $1,\ldots,M$; E_ν and E_μ are the levels of the required and the unperturbed potential wells; $\Psi_0^T(r) = \{\Psi_0(E_\nu,r),\ldots,\Psi_0(E_{\mu'},r)\ldots\}$ is the row vector of solutions of the original rectangular well; γ_ν and $\gamma_{0\mu}$ are the reduced widths of the bound states in the required well $V(x)$ and in the original well $V_0(x)$, respectively (in the given case, they

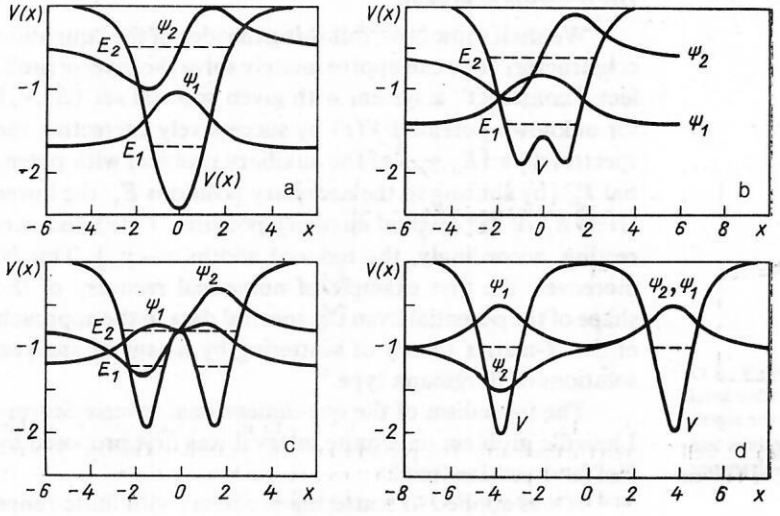

FIG. 12. Gradual change in the shape of a transparent potential well [from (a) to (d)] as the levels of two of its bound states approach each other. The deformation of the wave functions is also shown.[76]

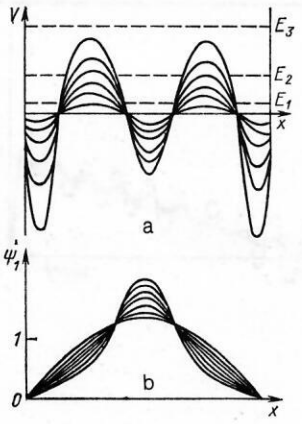

FIG. 13. Perturbations due to raising of the second level to the third: a) deformation of the potential as $E_1 \to E_3$; the barriers in the region of the maxima of $|\Psi_2|(x)$ push E_2 upward, overpowering the influence of the attractive wells near the nodes of Ψ_2; the form of the corresponding wave functions is not shown, but qualitative conclusions about them can be drawn by examining the second and third eigenfunctions in Fig. 14; b) the ground-state functions corresponding to the potentials shown in Fig. 1a.

are included in the values of the eigenfunctions and do not occur explicitly); T is the symbol of the transpose; $\hat{P}(r)$ is a 2×2 block matrix with elements of the four blocks[52]

$$\left.\begin{aligned} P_{\nu'\nu}(r) &= \delta_{\nu'\nu} + \int_r^a \Psi(E_{\nu'}, r')\,\Psi(E_\nu, r')\,dr';\\ P_{\nu'\mu}(r) &= \int_r^a \Psi(E_{\nu'}, r')\,\Psi(E_\mu, r')\,dr';\\ P_{\mu'\nu}(r) &= -\int_r^a \Psi(E_{\mu'}, r')\,\Psi(E_\nu, r')\,dr';\\ P_{\mu'\mu}(r) &= \delta_{\mu'\mu} - \int_r^a \Psi(E_{\mu'}, r')\,\Psi(E_\mu, r')\,dr'. \end{aligned}\right\} \qquad (3)$$

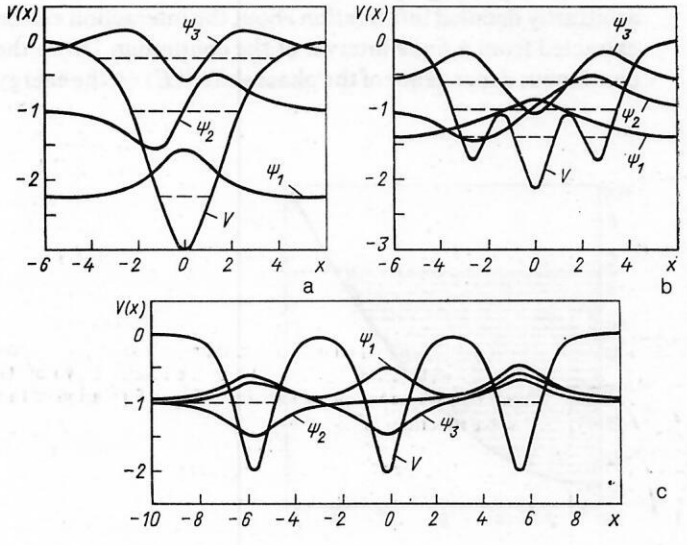

FIG. 14. Gradual change in the shape of a transparent potential well [from (a) to (c)] when three levels approach each other. The broken lines show the levels.[76]

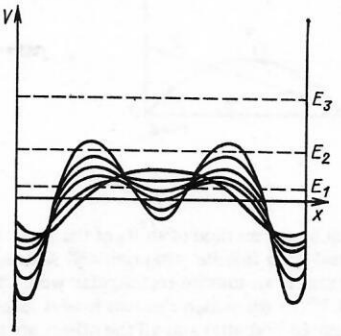

FIG. 15. Superposition of perturbations when $E_1 \to E_2 \to E_3$. The series of potential corrections to the infinite rectangular well shift the ground level to E_2, and E_2 to E_3. The form of the perturbation is "made up" from the elementary perturbations shown in Figs. 10a and 13a.

The potential that is recovered in the M-level approximation has the form[52]

$$\begin{aligned} V(r) = 2\Big\{ &\sum_{\nu\nu'} \Psi(E_\nu, r)\,P^{-1}_{\nu\nu'}(r)\,\Psi(E_{\nu'}, r)\\ &-\sum_{\nu\mu'} \Psi(E_\nu, r)\,P^{-1}_{\nu\mu'}(r)\,\Psi_0(E_{\mu'}, r)\\ &+\sum_{\mu\nu'} \Psi_0(E_\mu, r)\,P^{-1}_{\mu\nu'}(r)\,\Psi(E_{\nu'}, r)\\ &-\sum_{\mu\mu'} \Psi_0(E_\mu, r)\,P^{-1}_{\mu\mu'}(r)\,\Psi_0(E_{\mu'}, r)\Big\}'. \end{aligned} \qquad (4)$$

As the required potential we took one with infinite walls at the ends of the interval $0 < r < a$ and a linear inclined bottom.

We first solved the auxiliary direct problem: with the potential that must be recovered we found the eigenvalues E_ν and the reduced widths γ_ν—the initial data for the inverse problem. Then in the infinite rectangular potential well the levels E_μ of a finite number of the lowest states were shifted to the positions of the given values E_ν, and the values of their reduced widths γ_μ were replaced by γ_ν. The rectangular well was deformed and approached the required potential.

Figues 17–19 show the shapes of the potentials of Barg-

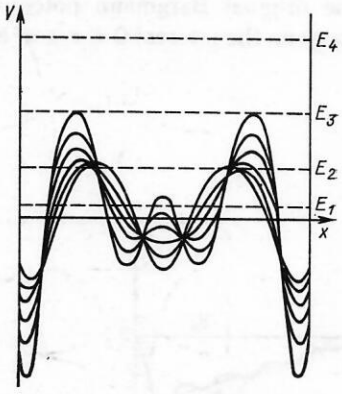

FIG. 16. The same as in Fig. 15, but with an additional shift of the third level to the fourth. To a perturbation of the type shown in Fig. 15 there is "added" a perturbation with three maxima between the nodes of $\Psi_3(x)$ and three wells in the region of its nodes.

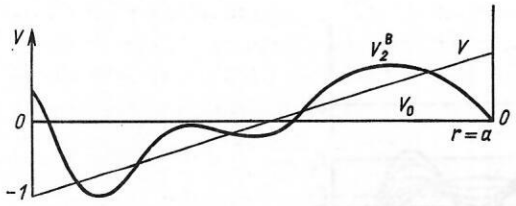

FIG. 17. Recovery of the potential by the method of shifts of the spectral parameters. The required potential is an infinite potential well with inclined bottom; the original potential is an infinite rectangular well; the curve is the Bargmann potential $V^B(r)$ for which the two lowest levels have the same $\{E_\nu,\gamma_\nu\}$ as the required potential and all the others are as for the unperturbed well (two-level approximate solution of the inverse problem).

mann type constructed from 2, 10, and 18 pairs of spectral parameters $\{E_\lambda,\gamma_\lambda\}$ for the lowest R-matrix states. It can be seen that initially there is a convergence of the successive approximations to the required potential, but that with further increase in the number of R resonances taken into account the errors of the calculations increase, and the oscillations of the approximate $V^B(r)$ relative to the line of the required potential become stronger.

To investigate the convergence of the approximate solutions of the inverse problems (particularly multichannel ones) it is helpful to have models that use exact analytic solutions of the direct problems as well. One can use a combination of the two different approaches (R-matrix approach and the approach of Gel'fand and Levitan or Marchenko) for construction of exactly solvable models in such a way that the model potentials obtained in the one approach are used as original potentials, while the Bargmann-type potentials of the other approach are used for approximate solution of the inverse problem. For example, we take a Bargmann potential and the corresponding solutions in the Gel'fand–Levitan or Marchenko approach and construct from these solutions wave functions that satisfy the Sturm–Liouville boundary conditions (of R-matrix resonance states). Thus, for the regular Bargmann solutions $\Phi(k,r)$, which are equal to zero at the origin and are known in analytic form, we find the values of $k = k_\nu$ and, thus, the energies at which they also vanish at the point $r = a$; this is a task appreciably simpler than numerical solution of a Schrödinger equation. From the E_ν and corresponding γ_ν found in this manner we approximately recover the original Bargmann potential (Gel'fand–Levitan), but only on the interval $0 \leqslant r \leqslant a$, by

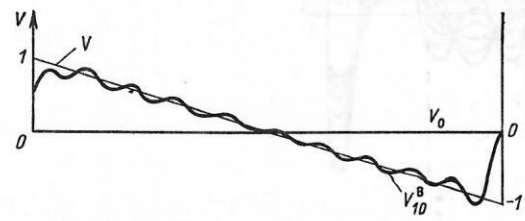

FIG. 18. The same as in Fig. 17, but the curve represents the $V^B(r)$ constructed from ten pairs of spectral parameters $\{E_\nu,\gamma_\nu\}$ of the required potential.

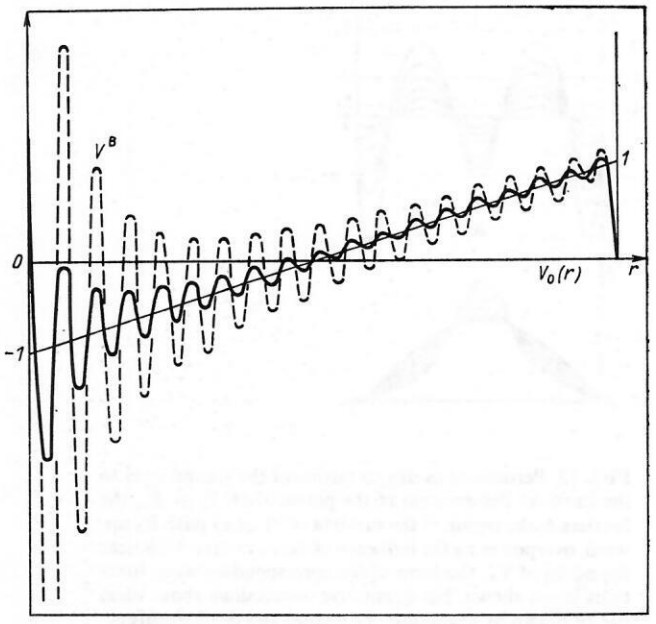

FIG. 19. The Bargmann potential constructed from 18 levels of the required well. The broken curve corresponds to the same accuracy of calculation of the spectral parameters $\{E_\nu,\gamma_\nu\}$ of the required potential as in Figs. 17 and 18; the continuous curve is obtained for the $V^B(r)$ recovered from $\{E_\nu,\gamma_\nu\}$ found by solving the direct problem with greater accuracy (with half the step of the difference differentiation).

means of the R-matrix Bargmann potentials, as shown above.

We proceed similarly in the multichannel case, using the matrix generalization of the procedure.

By virtue of the effectively unlimited accuracy with which one can determine the spectral parameters of the R-matrix problem from the exact Bargmann solutions of the Gel'fand–Levitan and Marchenko approach a way is thus opened to investigate the dependence of the errors with which the interaction is recovered on the degree of accuracy of specification of E_ν and the reduced widths.

For finite-range potentials that are bounded in value, arbitrarily detailed information about the interaction can be extracted from a *finite* interval of the continuum [from the continuous dependence of the phase shift $\delta(E)$ on the energy

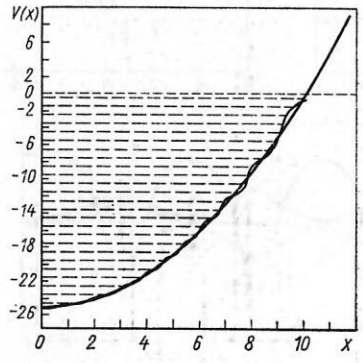

FIG. 20. Approximation of a reflectionless potential with 25 levels to the shape of an oscillator potential well when their spectra are identical in the region $E \leqslant E_{25}$ (Ref. 76).

one can determine a countable set of parameters E_ν, γ_ν, though it is true that uniqueness of the determination may here be hindered by the nonlinearity of the connection between $R(E)$ and E_ν, γ_ν].

Recovery of the shape of potentials by means of Bargmann potentials of finite depth

In 1980, Schonfeld *et al.*[86] showed (see also Ref. 75) how, by fitting up to eight levels of transparent "multisoliton" (reflectionless) potentials to the lower part of the spectra of linear, rectangular, and oscillator wells, one can approximately reproduce their shape in the region of energies in which the spectra of the approximated and the approximating potentials coincide. Later,[76] these authors made calculations with a larger number of levels. Figure 20 shows the approximation of an oscillator well by a transparent well for 25 coincident lowest levels and a special choice of the position of the upper edge of the finite well. It is remarkable that despite the completely different spectra (discrete and continuous) above these 25 levels such close coincidence of the shapes of the potentials for $E < E_{25}$ is obtained. Figure 20 is a new example of the reaction of the shape of the potential to a special kind of shift of the levels, which, as it were, "separate" from the lower edge of the continuum and sink to their specified equidistant positions (the actual position of the edge is cardinally important for the quality of the approximation). In Sec. 2, we shall consider examples of the shift of levels in the opposite direction: from the discrete spectrum to the continuum—immersion of bound states in the continuum (with potentials that keep the bound states above the decay threshold). These examples enable us to understand better *what regulates the transparency or the trapping properties of quantum systems with potential interaction*. In the next subsection, we discuss the effects of tunneling through potential barriers, which have a direct bearing on this.

Surprises on quantum tunneling

Resonance tunneling

A system of two identical potential barriers can be transparent at the energy of a quasistationary state between

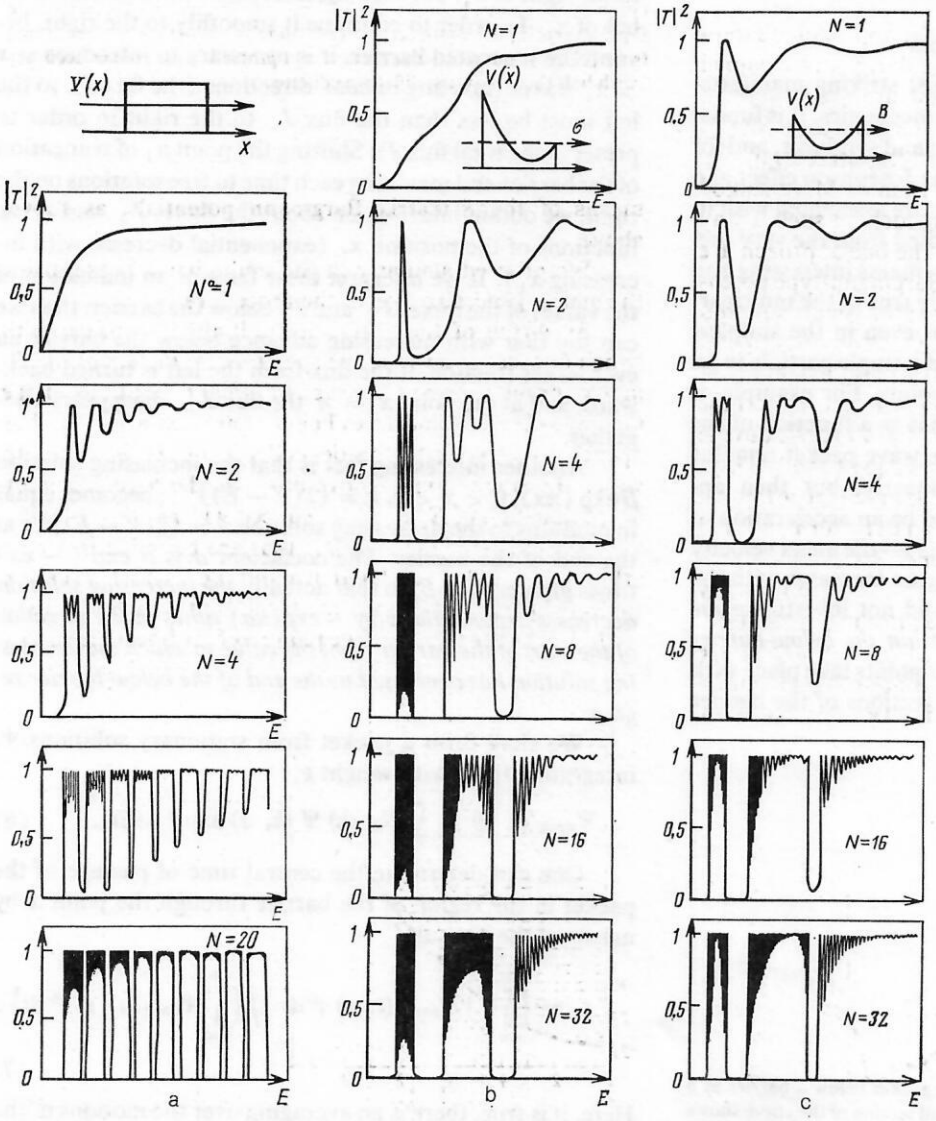

FIG. 21. Penetrability of a system of identical barriers for successive increase of their number: $N = 1, 2, 4, \ldots$: a) rectangular barriers; b), c) barriers with variable height.

them even if each of them separately is weakly penetrable. A simple explanation of this is given in Ref. 20; here we give another admittedly less rigorous explanation.

We imagine a standing wave trapped between barriers at a resonance energy. In both directions from the system of barriers there will propagate waves, with very small amplitudes, that have tunneled as a result of decay of the quasibound state. It is now sufficient if from one direction we direct toward such a system a weak incident wave with the same energy and with phase and amplitude such that the reflected wave to which it gives rise interferes with the decay wave and annihilates it; then in this way we obtain the required picture of transparency of the two barriers. Our treatment lacks rigor because we add solutions with energies that differ by a small imaginary correction. However, the essence of the phenomenon is correctly reproduced, and when the barriers are increased this inaccuracy can be made negligibly small.

Figure 21 shows the energy dependence of the penetrability coefficients for systems with different numbers N of identical barriers.[72] It can be seen how gradually, with increasing N, bands of allowed motion of a one-dimensional crystal lattice (conduction bands) are formed.

Velocity of a wave packet below a barrier

Below-barrier tunneling is a most striking manifestation of the specific nature of quantum mechanics. It is fundamentally important for nuclear fission and synthesis, and for the majority of nuclear reactions. The Josephson effect and the creation of the tunnel microscope are associated with it. But although tunneling has been studied from the very creation of quantum theory, much in it remains interesting and poorly understood. This is particularly true of the multiparticle aspects of the phenomenon, but even in the simplest one-dimensional case of the motion of a single particle in an external field there are mysterious points. For example, it was found by Fletcher[63] (Fig. 22) that as a function of the barrier width A the time t_A that the wave packet remains below the barrier first increases linearly, but then approaches saturation. There appears to be an acceleration of waves as they pass through long barriers—the mean velocity of the motion in the below-barrier region increases with the length of the barrier. But Fletcher did not investigate *the time evolution of the wave packet within the below-barrier region*. Does the motion at its different points take place with the same velocity, or are individual sections of the barrier traversed more rapidly (or more slowly)? In Ref. 91, estimates were made of the times at which the "center of mass" of the packet or its maximum are at different points of the below-barrier region. It was found that the motion is exponentially decelerated in the direction from the beginning to the end of the barrier, so that the time required to pass through the below-barrier region is mainly taken at the end of the barrier.

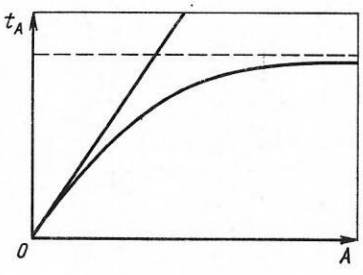

FIG. 22. Time dependence of delay t_A of a packet below a barrier as a function of the barrier width A. The horizontal section of the curve shows that for a sufficiently long barrier an additional increase of its width does not lead to a further loss of time on tunneling through it. The inclined line corresponds to a constant finite velocity of the packet.

We consider first the simplest case of a rectangular barrier. The flux

$$J = \mathrm{i}/2m\,[\Psi(x)\,\Psi^{*\prime}(x) - \Psi^{*}(x)\,\Psi^{\prime}(x)] \qquad (5)$$

has, in accordance with the law of its conservation, a constant value before, within, and after the barrier. Before the barrier it is the sum of the fluxes of the incident and reflected waves. Less well known is the fact that *within the barrier the fluxes for the individual components of the solution (increasing and decreasing) are equal to zero, and it is only their interference that ensures conservation of* J.

Formally, one could speak of fluxes traveling in opposite directions below the barrier at an arbitrary point x_1. Let us shorten the barrier, removing the part of it that is situated to the right of x_1, but keeping unchanged the solution to the left of x_1. In order to continue it smoothly to the right, beyond the truncated barrier, it is necessary to introduce at $x > x_1$ waves traveling *in both* directions (the flux J_- to the left must be less than the flux J_+ to the right in order to preserve the total flux J). Shifting the point x_1 of truncation of the barrier and matching each time to free solutions on the right, we obtain information about the fluxes J_+ and J_- as functions of the position x_1 (exponential decrease with increasing x_1). If we interpret these facts as an indication of the values of the fluxes J_+ and J_- below the barrier, then we can say that with increasing advance below the barrier an ever larger fraction of the flux from the left is turned backward, and at the point $x = A$ the flux J_+ disappears altogether.

Another interesting fact is that the increasing solution $\beta \exp(\varkappa x)$, $0 < x < a$, $\varkappa = \{2(V-E)\}^{1/2}$; becomes equal in modulus to the decreasing solution $\varkappa = \{2(V-E)\}^{1/2}$ at the end of the barrier. The coefficient α is $\alpha \exp(-\varkappa x)$ times greater than β, so that actually *the increasing solution decreases exponentially by* $\sim \exp(\varkappa a)$ *times in the direction of the start of the barrier from the value to which the decreasing solution has decreased at the end of the below-barrier region.*

We shall form a packet from stationary solutions Ψ, integrating them with weight g_k:

$$\Psi_{\mathrm{pack}}(t, x) = \int dk g(k)\,\Psi(k, x)\exp(-\mathrm{i}Et). \qquad (6)$$

One can determine the central time of passage of the packet in the region of the barrier through the point x by means of the formula[33]

$$t_x = \left\{\int_{-\infty}^{\infty} t\,|\,\Psi_{\mathrm{pack}}(t, x)\,|^2\,dt\right\} \Big/ \left\{\int_{-\infty}^{\infty} |\Psi_{\mathrm{pack}}(t, x)\,|^2\,dt\right\}. \qquad (7)$$

Here, it is true, there is an averaging over the motions of the waves in the two directions.

Figure 23 shows the dependence t_x for barriers of differ-

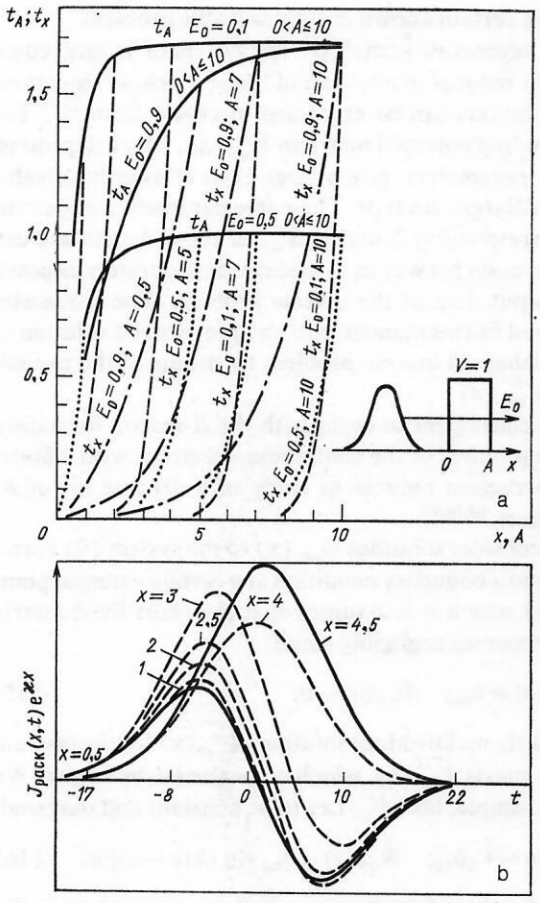

FIG. 23. Time evolution of a wave packet below the barrier: a) the times t_x of passage of the "center of mass" of the packet through the point x as functions of the position of this point below the barrier, $0<x\leqslant A$, for different values of the mean energy E_0 of the packet; the broken curve corresponds to $E_0 = 0.1$ V, the dotted curve to $E_0 = 0.5$ V, and the chain curve to $E_0 = 0.9$ V; the dependence of the times t_A of delay of the packet by the barrier on the barrier width is shown by the continuous curve; b) the time dependence of the mean flux at points $(0<x<5)$ below a barrier having width $A = 5$; for convenience of comparison of the values of the fluxes $J_{\text{pack}}(x,t) = (i/2m)[\Psi^*_{\text{pack}}(x,t)\Psi'_{\text{pack}}(x,t) - \Psi_{\text{pack}}(x,t)\Psi'^*_{\text{pack}}(x,t)]$ at different points they are shown with multiplication by $\exp(\varkappa x)$.

ent lengths A, and Fig. 23b shows the time dependence of the flux $J_{\text{pack}}(x,t)$ at different points x below the barrier. The positive and negative total fluxes seen shifted in time in Fig. 23b are apparently the first direct proof of the presence of the incident and reflected components of the packet in the below-barrier region. For better comparison of the time evolution $J_{\text{pack}}(x,t)$ at different points x, we have introduced in Fig. 23b factors $\exp(\varkappa x)$, which compensate the exponential damping (with increasing x) of the waves below the barrier.

All the curves in Fig. 23a emanate from the zero point. But this occurs only if we measure t_x and t_A from the time t_0 when the center of the complete packet (with incident and reflected components—the latter has an appreciable time delay) is situated at the point $x = 0$.

The steep rise of the curves t_x at the end of the barrier and the displacement of the maximum of $J_{\text{pack}}(x,t)$ in Fig. 23b correspond to damping of the velocity of the packet below the barrier as it approaches $x = A$.

These calculations agree with the results of Fletcher[63] both in showing that the delay time t_A for sufficiently wide barriers ceases to depend on A and in showing that these saturated delay times are minimal when the mean energy of the packet is equal to half the height of the barrier. For wide barriers, there is an analytic expression for this dependence:

$$t_A = \hbar\,[E\,(V - E)]^{-1/2}.$$

2. MULTICHANNEL EQUATIONS

Nonrelativistic quantum physics is already to a large degree a multichannel physics, and in the future this tendency will be rapidly enhanced. Multichannel problems often have a direct physical significance. They are also interesting because multidimensional problems reduce to them—it is more convenient to solve a system of ordinary differential equations (coupled one-dimensional Schrödinger equations) than to solve partial differential equations.

Multichannel equations are particularly interesting in their connection with multiparticle problems. The latter are difficult both on account of their multidimensional nature and in the complexity of the regions of interaction in the multidimensional configuration space. As an illustration, we show in the Appendix the *picture of the regions of interaction of four particles* moving along one axis (we decided to show it, since we have never encountered it in the literature, and few physicists can have formed a clear idea of it; it is published here for the first time).

We begin with the example of the reduction of the simplest one-dimensional system of three bodies to multichannel one-dimensional equations.

If exactly solvable models deepen our qualitative understanding of the properties of single-channel quantum objects, the need for exactly solvable examples is immeasurably greater for complicated systems with strong channel coupling, for which our quantum intuition is much weaker. To facilitate the use of the multichannel models and free them, for those who may need the models, from calculations that are cumbersome rather than inherently difficult and to reduce to a minimum the possible errors in the formulas, we give them here for finite-range interactions (in the framework of R-matrix theory) in a general and, as far as possible, compact form, following Ref. 52 with certain improvements.

We shall discuss models with a separation of the variables—with an ordinary continuous coordinate of the configuration space and a variable of *the motion through the "lattice of channels" in a multichannel problem or through a "lattice of periods" in a periodic field.*

At the end of the section, we shall consider the deformation of the interaction matrix $V_{\alpha\beta}(x)$ of an exactly solvable model problem when a bound state is shifted into the continuum. We shall compare the single-channel and multichannel cases.

Multiparticle and multichannel inverse problem

Reduction of a three-particle problem to a multichannel problem

Suppose that particle 1 is scattered by a composite target, namely, particle 2, which is confined in an infinite rectangular potential well near particle 3, which is fixed at the point $x = 0$. The picture of the interaction regions in this case differs from the one shown in Fig. A1 in that only mo-

tion in the horizontal strip is allowed.

The corresponding Schrödinger (partial differential) equation

$$[-\partial^2/\partial x_1^2 - \partial^2/\partial x_2^2 + V_1(x_1) + V_2(x_2) + V_{12}(|x_1 - x_2|) + V_{123}(x_1, x_2)]\Psi(x_1, x_2) = E\Psi(x_1, x_2) \quad (8)$$

can be reduced to the system of ordinary differential equations

$$-\frac{d^2}{dx_1^2}\Psi_\alpha(x_1) + V_1(x_1) + \sum_\beta V_{\alpha\beta}(x_1)\Psi_\beta(x_1) = (E - \varepsilon_\alpha)\Psi_\alpha(x_1) \quad (9)$$

for the coefficients $\Psi_\alpha(x_1)$ of the expansion

$$\Psi(x_1, x_2) = \sum_\alpha \Psi_\alpha(x_1)\Phi_\alpha(x_2) \quad (10)$$

of the three-body wave function into a complete set of states $\Phi_\alpha(x_2)$ of the internal motion of the target:

$$-\frac{d^2}{dx_2^2}\Phi_\alpha(x_2) + V_2(x_2)\Phi_\alpha(x_2) = \varepsilon_\alpha\Phi_\alpha(x_2). \quad (11)$$

The potential matrix $V_{\alpha\beta}(x_1)$, which couples the equations in the system (9), can be expressed in terms of the potential $V_{12}(x_1 - x_2)$ and the three-particle potential $V_{123}(|x_1, x_2|)$ if it is not equal to zero:

$$V_{\alpha\beta}(x_1) = \int \Phi_\alpha(x_2)[V_{12}(|x_1 - x_2|) + V_{123}(x_1, x_2)]\Phi_\beta(x_2)\,dx_2. \quad (12)$$

The system of multichannel equations (9) can, in particular, be used to solve the three-particle inverse problem.[90,94] If the two-particle potentials V_1, V_2, and V_{12} are assumed to be known, then, by recovering the matrix $V_{\alpha\beta}(x_1)$ from the scattering data, we can find the unknown potential $V_{123}(x_1, x_2)$ by inverting the relation (12).

Multichannel inverse problem

We first construct exactly solvable models for the M-channel system which can be obtained by truncating the system (9).

To the system of M coupled one-dimensional Schrödinger equations there corresponds a system of equations of the inverse problem that is the matrix generalization (Refs. 20, 52, and 82) of the ordinary Gel'fand–Levitan–Marchenko equation (for simplicity, we shall omit the indices 1 of the spatial variables x, y, z of the first particle):

$$K_{\alpha\alpha'}(x, y) + Q_{\alpha\alpha'}(x, y) + \int_x^a dz \sum_{\beta=1}^M K_{\alpha\beta}(x, z)Q_{\beta\alpha'}(z, y) = 0, \quad (13)$$

where the matrix kernel Q is determined by the original spectral (or scattering) data, and the matrix solution K of Eq. (13) determines the required potential matrix:

$$V_{\alpha\beta}(x) = \mathring{V}_{\alpha\beta}(x) - 2\frac{d}{dx}[K_{\alpha\beta}(x, x)]. \quad (14)$$

The minus sign in Eq. (14) and the limits of the integral in (13) are chosen in accordance with the R-matrix version of the formalism of the inverse problem (see Ref. 20). By the symbol $\circ$ we denote the functions $\mathring{V}_{\alpha\beta}(x)$, etc., that correspond to a certain known exactly solvable problem.

For degenerate kernels Q^B, the system of integral equations (13) reduces to a system of linear algebraic equations whose solutions can be expressed in closed form.[20,82] The corresponding potential matrices $V^B_{\alpha\beta}(x)$, which depend on arbitrary parameters, give a large class of exactly solvable models of Bargmann type. These free parameters also occur in the corresponding S matrix $S^B_{\alpha\beta}$ or the R matrix and can be chosen in such a way as to describe as accurately as possible the input data of the inverse problem. The parameter values fixed in this manner give an approximate solution of the multichannel inverse problem by means of the explicit form of $V^B_{\alpha\beta}(x)$.

It is convenient to begin with the R-matrix formalism when the problem of the continuous spectrum with a finite-range interaction reduces to study of a discrete set of R-matrix states.[14,20,28]

We consider solutions $\Phi_{\alpha\beta}(x)$ of the system (9) corresponding to a boundary condition at a certain external point $x = a$, at which it is assumed that the short-lived matrix $V_{\alpha\beta}(x)$ becomes negligibly small

$$\Phi'_{\alpha\beta}(a) = \delta_{\alpha\beta}; \quad \Phi_{\alpha\beta}(a) = 0, \quad (15)$$

and similarly we introduce solutions $\mathring{\Phi}_{\alpha\beta}(x)$ for the original potential matrix $\mathring{V}_{\alpha\beta}(x)$, which is assumed to be known. We can, for example, take $\mathring{V}_{\alpha\beta}(x)$ to be constant and diagonal:

$$\mathring{V}_{\alpha\beta}(x) = \mathring{V}_\alpha\delta_{\alpha\beta}; \quad \mathring{\Phi}_{\alpha\beta}(x) = \delta_{\alpha\beta}\sin[k(x-a)]/k. \quad (16)$$

Besides these functions, we shall use eigensolutions $\Psi^\nu_\alpha(x) = \Psi_\alpha(E^\nu, x)$ for Eq. (9) and $\mathring{\Psi}\mu_{\alpha\beta}(x) = \mathring{\Psi}_\alpha(\mathring{E}^\mu, x)$ for the reference interaction matrix $\mathring{V}_{\alpha\beta}(x)$ with boundary conditions

$$\Psi^\nu_\alpha(0) = \mathring{\Psi}^\mu_\alpha(0) = 0; \quad \Psi^\nu_\alpha(a) = \mathring{\Psi}^\mu_\alpha(a) = 0. \quad (17)$$

These eigenfunctions are assumed to be normalized,

$$\sum_{\alpha=1}^M \int_0^a [\Psi^\nu_\alpha(x)]^2\,dx = 1; \quad \sum_{\alpha=1}^M \int_0^a [\mathring{\Psi}^\mu_\alpha(x)]^2\,dx = 1, \quad (18)$$

and can be represented in the form of linear combinations of the functions $\Phi_{\alpha\beta}(x)$ and $\mathring{\Phi}_{\alpha\beta}(x)$ for energy eigenvalues E^ν and $\mathring{E}^\mu$:

$$\left.\begin{aligned}\Psi^\nu_\alpha(x) &= \sum_{\beta=1}^M \Phi_{\alpha\beta}(E^\nu, x)\Gamma^\nu_\beta;\\ \mathring{\Psi}^\mu_\alpha(x) &= \sum_{\beta=1}^M \mathring{\Phi}_{\alpha\beta}(\mathring{E}^\mu, x)\mathring{\Gamma}^\mu_\beta,\end{aligned}\right\} \quad (19)$$

where the coefficients Γ (the components of the normalization vectors) are determined by the boundary values of the derivatives of the eigenvectors Ψ:

$$\Gamma^\nu_\alpha = [\Psi^\nu_\alpha]'_{x=a}; \quad \mathring{\Gamma}^\mu_\alpha = [\mathring{\Psi}^\mu_\alpha]'_{x=a}. \quad (20)$$

We shall also need vectors of solutions of the system (9) with the reference potential matrix $\mathring{V}_{\alpha\beta}(x)$, constructed by analogy with (19) but for energy values $E = E^\nu$ that correspond to the required potential matrix $V_{\alpha\beta}(x)$:

$$\mathring{\Psi}^\nu_\alpha(x) = \sum_{\beta=1}^M \mathring{\Phi}_{\alpha\beta}(E^\nu, x)\Gamma^\nu_\beta. \quad (21)$$

By means of the vectors (19) and (21), we can con-

struct the degenerate kernel Q of the integral equation (13) and the K corresponding to it:

$$Q^{\mathrm{B}}_{\alpha\beta}(x,\ y)=\sum_{\nu=1}^{M}\mathring{\Psi}^{\nu}_{\alpha}(x)\,\mathring{\Psi}^{\nu}_{\beta}(y)-\sum_{1}^{M}\mathring{\Psi}^{\mu}_{\alpha}(x)\,\mathring{\Psi}^{\mu}_{\beta}(y); \tag{22}$$

$$K^{\mathrm{B}}_{\alpha\beta}(x,\ y)=-\sum_{\nu=1}^{M}\Psi^{\nu}_{\alpha}(x)\,\mathring{\Psi}^{\nu}_{\beta}(y)+\sum_{\mu=1}^{M}\Psi^{\mu}_{\alpha}(x)\,\mathring{\Psi}^{\mu}_{\beta}(y). \tag{23}$$

These expressions can also be written in a more compact form as scalar products:

$$Q(x,\ y)=\hat{\Psi}^{t\tau}_{0}(x)\,\hat{\Psi}^{T-}_{0}(y); \tag{22'}$$

$$K(x,\ y)=-\hat{\Psi}^{t\tau}(x)\,\hat{\Psi}^{T-}_{0}(y), \tag{23'}$$

where the symbol $\hat{}$ on Ψ denotes a vector in three (or two) "spaces" with components labeled by the channel index α, by the superscripts ν or μ and one omitted index that indicates the connection of the given component to the parameters of the original subspace of the group (μ), for example, $\mathring{V}_{\alpha\beta}(x)$ or the required subspace of the group (ν) of the interaction $\mathring{V}_{\alpha\beta}(x)$. The superscripts T, t, τ denote the corresponding transpose of the vectors in these "spaces." For simplicity, we shall omit in the majority of cases the variable x in the arguments of the functions

$$\hat{\Psi}^{t\tau}(x)=\left\{\begin{bmatrix}(\Psi^{\nu=1}_{\alpha=1}(x);&\Psi^{\nu=2}_{\alpha=1};&\ldots;&\Psi^{\nu=M}_{\alpha=1})\\(\Psi^{\nu=1}_{\alpha=2}(x);&\Psi^{\nu=2}_{\alpha=2};&\ldots;&\Psi^{\nu=M}_{\alpha=2})\\\cdots&\cdots&\cdots&\cdots\\(\Psi^{\nu=1}_{\alpha=M}(x);&\Psi^{\nu=2}_{\alpha=M};&\ldots;&\Psi^{\nu=M}_{\alpha=M})\end{bmatrix}\right.$$

$$\left.\times\begin{bmatrix}(\Psi^{\mu=1}_{\alpha=1};&\Psi^{\mu=2}_{\alpha=1};&\ldots;&\Psi^{\mu=M}_{\alpha=1})\\(\Psi^{\mu=1}_{\alpha=2};&\Psi^{\mu=2}_{\alpha=2};&\ldots;&\Psi^{\mu=M}_{\alpha=2})\\\cdots&\cdots&\cdots&\cdots\\(\Psi^{\mu=1}_{\alpha=M};&\Psi^{\mu=2}_{\alpha=M};&\ldots;&\Psi^{\mu=M}_{\alpha=M})\end{bmatrix}\right\}$$

$$=\{\hat{\Psi}^{\nu t}(x),\ \hat{\Psi}^{\mu t}(x)\}.$$

This is a column vector with respect to the α components and a row vector with respect to the ν and μ components:

$$\hat{\Psi}^{T-}(y)$$

$$=\left\{\begin{bmatrix}\begin{bmatrix}\Psi^{\nu=1}_{\beta=1}(y)\\\Psi^{\nu=2}_{\beta=1}(y)\\\cdots\\\Psi^{\nu=M}_{\beta=1}(y)\end{bmatrix}&\begin{bmatrix}\Psi^{\nu=1}_{\beta=2}\\\Psi^{\nu=2}_{\beta=2}\\\cdots\\\Psi^{\mu=M}_{\beta=2}\end{bmatrix}&\cdots&\begin{bmatrix}\Psi^{\nu=1}_{\beta=M}\\\Psi^{\nu=2}_{\beta=M}\\\cdots\\\Psi^{\nu=M}_{\beta=M}\end{bmatrix}\end{bmatrix}\right.$$

$$\left.-\begin{bmatrix}\begin{bmatrix}\Psi^{\mu=1}_{\beta=1}(y)\\\Psi^{\mu=2}_{\beta=1}(y)\\\cdots\\\Psi^{\mu=M}_{\beta=1}(y)\end{bmatrix}&\begin{bmatrix}\Psi^{\mu=1}_{\beta=2}\\\Psi^{\mu=2}_{\beta=2}\\\cdots\\\Psi^{\mu=M}_{\beta=2}\end{bmatrix}&\cdots&\begin{bmatrix}\Psi^{\mu=1}_{\beta=M}\\\Psi^{\mu=2}_{\beta=M}\\\cdots\\\Psi^{\mu=M}_{\beta=M}\end{bmatrix}\end{bmatrix}\right\}$$

$$=\begin{Bmatrix}\hat{\Psi}^{\nu T}(y)\\\hat{\Psi}^{\mu T}(y)\end{Bmatrix}.$$

The superscript $^-$ corresponds to the sign of the μ components of the vector (i.e., the μ vector). This is a row vector with respect to the α components and a column vector with respect to the ν and μ components. The vectors $\hat{\Psi}^{t\tau}_{0}(x)$ and $\hat{\Psi}^{T-}_{0}(x)$, which correspond to the reference matrix $\mathring{V}_{\alpha\beta}(x)$, have a similar form. The kernels K and Q do not have a ν–μ structure.

Substituting Q and K in the degenerate form (22)–(23) into the integral equation (13), we obtain algebraic equations for the eigenvectors $\hat{\Psi}$:

$$\hat{\Psi}^{t\tau}(x)\left[1+\int_{x}^{a}\hat{\Psi}^{T-}_{0}(y)\,\hat{\Psi}^{t\tau}_{0}(y)\,dy\right]=\hat{\Psi}^{t\tau}_{0}(x). \tag{24}$$

The solution of these equations can be expressed in a closed form

$$\hat{\Psi}^{t\tau}(x)=\hat{\Psi}^{t\tau}_{0}(x)\{P(x)\}^{-1}, \tag{25}$$

where $P(x)$ is a scalar in the space of the channel indices α and a matrix in the vector spaces, with components labeled by means of ν and μ:

$$P(x)=1+\int_{x}^{a}\hat{\Psi}^{T-}_{0}(y)\,\hat{\Psi}^{t\tau}_{0}(y)\,dy, \tag{26}$$

where the ν and μ structure of P is $\begin{bmatrix}\hat{P}^{\nu\nu'}\hat{P}^{\nu\mu'}\\\hat{P}^{\mu\nu'}\hat{P}^{\mu\mu'}\end{bmatrix}$.

The kernel $K^{\mathrm{B}}(x,y)$ can now be written in the form

$$K^{\mathrm{B}}(x,\ y)=-\{\hat{\Psi}^{t\tau}_{0}(x)[P(x)]^{-1},\ \hat{\Psi}^{T-}_{0}(y)\}, \tag{23''}$$

and for equal arguments [cf. Eq. (4.1.9) in the book of Chadan and Sabatier[57]] as

$$\hat{K}^{\mathrm{B}}(x,\ x)=\mathrm{Sp}\{\hat{\Psi}^{T-}_{0}(x)\,P^{-1}(x)\,\hat{\Psi}^{t\tau}_{0}(x)\}$$
$$=\mathrm{Sp}\left\{P^{-1}(x)\frac{d}{dx}[P(x)]\right\}=\frac{d}{dx}[\ln\det P(x)]. \tag{23'''}$$

One of the conveniences of expressing the solutions in the explicit form (25) is the possibility of verifying (by direct substitution; see Ref. 52) that the matrix Schrödinger equation (9) with potential matrix obtained in accordance with (14),

$$\hat{V}(x)=2\{\hat{\Psi}^{t\tau}_{0}(x)\}'\{P(x)\}^{-1}\hat{\Psi}^{T-}_{0}(x)$$
$$-2\hat{\Psi}^{t\tau}_{0}(x)\,P^{-1}P'P^{-1}\hat{\Psi}^{T-}_{0}(x)$$
$$+2\hat{\Psi}^{t\tau}_{0}(x)\,P^{-1}\{\hat{\Psi}^{T-}_{0}(x)\}', \tag{27}$$

is satisfied by the function (25). In (27), we have used the rule for differentiating an inverse matrix:

$$\{P^{-1}\}=-P^{-1}P'P^{-1}. \tag{28}$$

Using (14) and (23'''), we obtain one further, more compact form of expression for the potential matrix [cf. Eq. (4.1.10) in Ref. 57):

$$\hat{V}(x)=-2\frac{d^2}{dx^2}[\ln\det P(x)], \tag{29}$$

$$P'=-\hat{\Psi}^{T-}_{0}(x)\,\hat{\Psi}^{t\tau}_{0}(x). \tag{30}$$

To verify the solution, we also take into account the Schrödinger equation for free motion,

$$-\{\hat{\Psi}^{t\tau}_{0}(x)\}''=\hat{\Psi}^{t\tau}_{0}(x)\,\hat{E};\quad -\{\hat{\Psi}^{T-}_{0}(x)\}''=\hat{E}\hat{\Psi}^{T-}_{0}(x), \tag{31}$$

and the fact that the Wronskian of the free solutions can be rewritten in the form (note the order of the factors on the right-hand side)

$$W=\int_x^a \hat{\Psi}_0^{T-}(y)\,\hat{\Psi}_0^{t\tau}(y)\,dy\hat{E}-\hat{E}\int_x^a \hat{\Psi}_0^{T-}(y)\,\hat{\Psi}_0^{t\tau}(y)\,dy, \quad (32)$$

where $\hat{E}$ is a diagonal $2MN\times 2MN$ matrix formed from the values of the energy $E^\nu-\varepsilon_\alpha$, $E^\mu-\varepsilon_\alpha$, and the integrals can be expressed in terms of P by means of Eq. (26),

$$W=(P-1)\,\hat{E}-\hat{E}\,(P-1). \quad (32')$$

To verify that the eigenfunction (25) satisfies the boundary conditions (17) and that its derivative is equal to $\hat{\Gamma}^{t\tau}$ at $x=a$, it is sufficient to take Eq. (24) for $x=0$, $x=a$ and the derivative of both sides of (24) at $x=a$. It is merely necessary to take into account the obvious fact that the integral in Eq. (26) vanishes in the limit $x\to a$, and also the orthonormalization condition for $\hat{\Psi}_0$ [thus, we have $\hat{P}^{\mu\mu'}(0)=1-1=0$ for the μ submatrix in P]. Therefore, in the μ-subvector component of Eq. (24),

$$\hat{\Psi}^\nu(x)\,\hat{P}^{\nu\mu}(x)+\hat{\Psi}^{\mu'}(x)\,\hat{P}^{\mu'\mu}(x)=\hat{\Psi}_0^\mu(x), \quad (33)$$

we have [$\hat{P}^{\mu\mu'}(0)=0$, see also Eq. (17)] at $x=0$:

$$\hat{\Psi}^\nu(0)\,\hat{P}^{\nu\mu}(0)=\hat{\Psi}_0^\mu(0)\equiv 0. \quad (33')$$

If $\hat{P}^{\nu\mu}$ is a square matrix, i.e., the dimensions of the ν and μ spaces are the same, Eq. (24′) gives $\hat{\Psi}^\nu(0)\equiv 0$, as the boundary conditions require. But if we had attempted to construct a model of a system with the same spectral data $[\hat{E};\hat{\Gamma}]$ as for the reference potential but with the addition of some new levels, the submatrix $\hat{P}^{\nu\mu}$ would not have been square and Eq. (24′) would not have ensured fulfillment of the boundary condition. Similarly, we cannot remove from the spectrum of the reference potential any levels without changing the spectral data of the other levels.

The ν component of Eq. (17) for $x=a$ gives

$$\hat{\Psi}^\nu(a)=\hat{\Psi}_0^\nu(a)=0;\ [\hat{\Psi}^\nu]'_{x=a}=[\hat{\Psi}_0^\nu]'_{x=a}=\hat{\Gamma}^\nu.$$

Representation of motion with respect to the channel-labeling variable α

In the complicated motion of the waves in a quantum multichannel system, it is possible to separate a simple but specific component. It turns out that one can readily construct exactly solvable models of motion with respect to a discrete variable α that labels the channels, obtaining discrete analogs of a rectangular well, Bargmann potentials, and others. As a result, the intuition acquired from the study of wave propagation in the ordinary configuration space is extended to the new dimension. In particular, there may exist resonances or bound states of a particular nature (corresponding to standing α waves).

A similar idea—to separate in the case of motion in a periodic field the free propagation of waves with respect to a discrete variable that labels the periods from the oscillations in each period—makes it possible to reexamine this most important quantum problem.

As we have already noted, the equations of motion for many complicated quantum systems are conveniently reduced to coupled one-dimensional Schrödinger equations with potential matrix $V_{\alpha,\alpha'}(x)$ and "channel functions" Ψ_α. Here, the indices α are variables conjugate to the spatial variables of the original multidimensional wave function, from which we have been able to "free" ourselves by means of a generalized Fourier transformation, leaving only one of them, x. The gain in computational simplicity (discreteness of the values of α and the possibility of making a restriction to a finite number of them) is, however, accompanied by a loss of physical transparency of the formalism. It is harder for us to picture the behavior of the channel functions in their dependence upon α than the form of a wave function in the ordinary space.

We shall show here that to a large degree transparency of the behavior of the functions in the α space can be restored. One can imagine motion with respect to α: oscillations, standing waves, resonances that cause scattering, and the propagation of packets in a nonstationary formulation of the problem. The key thing here is the "*separation" of the kinetic-energy operator of the α motion from the interaction matrix* $V_{\alpha,\beta}$. As a result, we obtain an ordinary Hamiltonian with respect to the new variable too. If in addition we choose a model potential energy that permits separation of the coordinates x and α, then we can obtain in pure form the channel component of the wave function and spectrum (bound states and resonances).

Such an approach was also unexpectedly found to be possible for quite different problems: motion of a particle in a periodic field. They will be considered below.

Model admitting separation of the variables x and α

We first make more precise what we mean by the term "channel." To describe complicated multidimensional and multiparticle quantum systems, it is convenient to expand the wave function $\Psi(x,\xi)$, which depends on several variables, with respect to known basis functions $\Phi_\alpha(\xi)$, where ξ denotes all the variables of the system except a *single* x, which is specially distinguished [expansion with respect to channels α; cf. Eq. (12)]:

$$\Psi(x,\xi)=\sum_\alpha \Psi_\alpha(x)\,\Phi_\alpha(\xi). \quad (34)$$

Substituting (34) in the Schrödinger equation and projecting this equation onto the various basis functions $\Phi_\alpha(\xi)$, we obtain a system of *one-dimensional* coupled Schrödinger equations for the coefficients Ψ_α of the expansion (34):

$$-\frac{d^2}{dx^2}\Psi_\alpha(x)+\sum_\beta V_{\alpha\beta}(x)\,\Psi_\beta(x)=(E-\varepsilon_\alpha)\,\Psi_\alpha(x). \quad (35)$$

In the system (35), waves can move with respect to the spatial variable x or can pass from one channel α to other channels β. It is usually simpler to solve one-dimensional systems of the type (35) on a computer than it is to solve the original differential Schrödinger equation. But the physical intuition about the details of the mechanism of the quantum processes that are determined by the interaction matrix $V_{\alpha\beta}(x)$ is as yet very poorly developed. One is forced to feed the initial data into the computer and obtain from it numerical results, forming hardly any idea of the qualitative connection between $V_{\alpha\beta}(x)$ and the spectral parameters or scattering data.

Exactly solvable models can here clarify the situation [enable us to look into the "black box" of the system (35)]. The simplest such models are those with δ-function and constant interaction matrices. Matrices of Bargmann type (see Ref. 20, Chap. 5) form a class of such solvable models.

In Ref. 91, a new approach was developed to the construction of exactly solvable models associated with *separation of the motion with respect to the spatial variable x and the channel variable α.*

It has now become clear that the difficulty of transferring our ordinary intuition about the motion of quantum waves in the x space to the motion with respect to α arises from the absence, in the multichannel Schrödinger operator of a *kinetic-energy operator* $\hat{T}_{\rm ch}$ *of displacement with respect to the channels.* Since the variable α is discrete, we construct such an operator as the finite-difference analog of the derivative of second order with respect to α (with step Δ):

$$\hat{T}_{\rm ch}\Psi_\alpha = -(\Psi_{\alpha+1}-2\Psi_\alpha+\Psi_{\alpha-1})/\Delta^2. \quad (36)$$

It can be assumed that $\hat{T}_{\rm ch}$ is contained in the interaction matrix $V_{\alpha\beta}$. We separate it [by adding and subtracting corresponding terms in (35) and including in the potential sum]:

$$-\frac{d^2}{dx^2}\Psi_\alpha(x)-(\Psi_{\alpha+1}-2\Psi_\alpha+\Psi_{\alpha-1})/\Delta^2 + \sum_\beta \tilde{V}_{\alpha\beta}(x)\Psi_\beta(x) = E\Psi_\alpha(x), \quad (37)$$

where the new effective interaction matrix $\tilde{V}_{\alpha\beta}(x)$ has the form

$$\tilde{V}_{\alpha\beta}(x) = V_{\alpha\beta}(x)+(\delta_{\alpha+1,\beta}-2\delta_{\alpha\beta}+\delta_{\alpha-1,\beta})/\Delta^2+\delta_{\alpha\beta}\varepsilon_\alpha. \quad (38)$$

Equation (37) is an equation in partial derivatives (ordinary ones with respect to x and difference ones with respect to α).

We now use the freedom in the choice of the matrix $V_{\alpha\beta}(x)$ and construct simple exactly solvable models in which motion with respect to the channel variable α is separated. For example, by a special choice of $V_{\alpha\beta}(x)$ we can obtain $\tilde{V}_{\alpha\beta}(x)$ in the form of a rectangular well,

$$\tilde{V}_{\alpha\beta}(x) = \delta_{\alpha\beta}V_0 \quad \text{for} \quad 0<x<R;\ 0<\alpha,\ \beta<M, \quad (39)$$

with an additional boundary condition that corresponds not only to a trapping infinite well but also to R-matrix scattering theory:

$$\Psi_\alpha(x) = 0 \quad \text{for} \quad x\leqslant 0,\ x\geqslant R,\ \alpha\leqslant 0,\ \alpha>M. \quad (40)$$

Here, by choosing a finite number M we have limited the number of coupled channels. The two-dimensional region, continuous with respect to x and discrete with respect to α, in which we seek the solution is shown in Fig. 24.

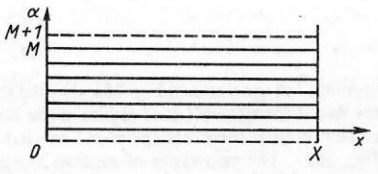

FIG. 24. Two-dimensional rectangular region in the (α,x) space in which the motion is described by the differential equation (4) in *partial derivatives.* The variable α takes discrete values, and x takes continuous values. The missing channels with $\alpha = 0$ and $\alpha = M+1$ are shown by the broken lines ($\Psi_{\alpha,0} = \Psi_{\alpha,M+1} = 0$).

To ensure fulfillment of the condition (39), the interaction matrix $V_{\alpha\beta}$ must also be tridiagonal [see (38), (39)]:

$$V_{\alpha\beta}(x) = \delta_{\alpha\beta}V_0-(\delta_{\alpha+1,\beta}-2\delta_{\alpha\beta}+\delta_{\alpha-1,\beta})/\Delta^2-\delta_{\alpha\beta}\varepsilon_\alpha. \quad (41)$$

From this formula there follows an important qualitative conclusion: *The widths* $L = M\Delta$ *of the well with respect to the variable α is narrower, the stronger the coupling of the channels* [the step Δ occurs in the expression for L as a factor, whereas in the potential (41) it occurs in the denominator and is squared].

In the two-dimensional differential–difference equation (37) with interaction matrix from (39) and boundary conditions (40) the variables x and α separate [$\Psi_\alpha(x) = \Psi_n(x)\chi_{\alpha m}$]:

$$-\frac{d^2}{dx^2}\Psi_n(x)+V_0\Psi_n(x) = \varepsilon_n\Psi_n(x);$$
$$\Psi_n(0)=0;\ \Psi_n(R)=0; \quad (42)$$

$$-(\chi_{\alpha+1,m}-2\chi_{\alpha m}+\chi_{\alpha-1,m}) = \Delta^2\lambda_m\chi_{\alpha m};$$
$$\chi_{0m}=0,\ \chi_{M+1,m}=0. \quad (43)$$

Equation (42) has the ordinary spectrum of an infinite rectangular well, $\varepsilon_n = V_0 + n^2\pi^2/R^2$, and the difference eigenvalue problem (43) in the rectangular well with respect to the variable α has M energy levels

$$\lambda_m = [1-\cos(\pi m/M)]/\Delta^2,$$

which only for $m \ll M$ are close to the levels of the corresponding problem with continuous α:

$$\lambda_m \underset{m\ll M}{\longrightarrow} m^2n^2/L^2, \text{where} L = M\Delta^2.$$

The complete spectrum of the system is the sum of the spectra for the motions with respect to the variables x and α:

$$E_{nm} = \varepsilon_n + \lambda_m. \quad (44)$$

Varying the well widths R and L, we can compress and stretch the "system" of levels ε_n and λ_m; for example, by increasing L, we obtain above each level of oscillations with respect to x a "band" of excitations of oscillations with respect to α. Let us recall here a specific feature of the finite-difference spectrum of a rectangular well. In contrast to the differential problem, the distance between the levels increases with increasing excitation energy only up to $n = M/2$, and above that the levels begin to get closer together (the spectrum is symmetric about its center).

In R-matrix scattering theory, these levels correspond to resonances (the only difference is that in R-matrix theory somewhat different boundary conditions for the eigenfunctions are used; see the paper of Lane and Thomas[28]). The idea that there could be resonances corresponding to α oscillations was first put forward by A. I. Baz', who also attempted to construct an exactly solvable model with such oscillations. However, the interaction matrix that he proposed did not admit separation of the variables x and α, and a kinetic-energy operator of the α motion was not separated in the Hamiltonian (see Ref. 1). This obscured the clarity of the physical picture. Several studies devoted to α resonances were made by Simonov *et al.*;[53] they called them *cc* (coupled-channel) resonances. In these studies too, the variables were not separated. But from the pedagogical point of view it is

preferable to introduce the concept of "channel" resonances by separating the variables of the configuration and channel spaces.

It is clear that not only the rectangular well but also other exactly solvable models can be generalized to the case of a channel variable (see Ref. 20). One can also consider cases of many channel variables, a continuum of channels, and a nonlocal coupling with respect to α (for example, interaction matrices separable with respect to α). We have shown above how one can separate from the potential matrix $V_{\alpha\beta}$ the operator of a second difference derivative (with tridiagonal matrix). To the difference derivatives of higher order (fourth, sixth, etc.) there correspond matrices with a larger number of diagonals (5, 7, *etc*). Whereas to the second-order (kinetic-energy) operator there correspond two linearly independent solutions, for example, waves traveling in opposite directions, to an operator of fourth order there correspond four independent waves [for example, $\exp(\pm ik_1 n)$, $\exp(\pm ik_2 n)$ for "free motion"; it should be noted that the relationship between the wave numbers k_1 and k_2 and the energy E is not the same as in the case of the ordinary Schrödinger equation; see Ref. 20)]. Similarly, for the sixth order there are six waves, etc. Thus, to a potential matrix of general form with all M diagonals nonzero there corresponds a complicated system of waves propagating through the "channel dimension." For matrices that depend on x the variables α and x do not separate, and there is a mixing of the oscillations with respect to α and x.

A further transparent model example of the participation of channel coupling in the formation of the spectrum of a system is provided by the difference (with respect to x: $x_n = n\cdot\Delta$) analog of the multichannel equations (35):

$$-[\Psi_\alpha(n+1)-2\Psi_\alpha(n)+\Psi_\alpha(n-1)]/\Delta^2+\sum_\beta V_{\alpha\beta}(n)\Psi_\beta(n) = (E-\varepsilon_\alpha)\Psi_\alpha(n). \quad (35')$$

If we impose homogeneous boundary conditions $\Psi_\alpha(0) = 0$, $\Psi_\alpha(N+1) = 0$, we obtain $M\times N$ homogeneous algebraic equations for the $M\times N$ unknowns $\Psi_\alpha(n)$ ($\alpha = 1, 2,..., M$; $n = 1, 2,..., N$), which have solutions for $N\times M$ energy eigenvalues, i.e., the spectrum is formed from N oscillatory states with respect to x_p and M with respect to α). *The convenience of this model with all discrete variables taking a finite number of values is the possibility of counting the points of the spectrum* (bound states and resonances) and seeing how their total number depends on the number of channels.

Motion from channel to channel in the special case of identical channels is directly related to the well-known phenomenon of the lifting of degeneracy by the inclusion of coupling between channels. Indeed, suppose that there are M uncoupled Schrödinger equations with identical potential wells and, therefore, with identical levels. If we regard these equations as a single system, the levels of its spectrum will be M-fold degenerate. But if we include a coupling of the channels (by introducing nondiagonal elements in the potential matrix), we split the levels, and this can be interpreted as the manifestation of a band of oscillatory excitations with respect to the channel variable α.

Bloch problem (band spectrum)

It turns out that the motion of a particle in a periodic external potential can also be considered from this point of view. We introduce the equivalent problem of motion in a two-dimensional (α,x) strip (ladder; see Fig. 25). For this, we first write down the equation for the motion of the particle on one of the periodic intervals (we denote it by the number α, which is equal to 0, ± 1, ± 2,...):

$$-\frac{d^2}{dx^2}\Psi_\alpha(x)+V(x)\Psi_\alpha(x)=E\Psi_\alpha(x);\ 0\leqslant x\leqslant X; \quad (45)$$

$$\Psi_\alpha(x)=\exp(i\gamma)\Psi_{\alpha+1}(x); \quad (46)$$

$$\Psi_\alpha(0)=\exp(i\gamma)\Psi_\alpha(X);\ \Psi'_\alpha(0)=\exp(i\gamma)\Psi'_\alpha(X). \quad (47)$$

We now add and subtract on the left-hand side of the Schrödinger equation a difference kinetic-energy operator of the type (36) ($X=\Delta$):

$$-\frac{d^2}{dx^2}\Psi_\alpha(x)+\hat{T}_{ch}\Psi_\alpha(x)+[\Psi_{\alpha+1}(x)-2\Psi_\alpha(x) +\Psi_{\alpha-1}(x)]/\Delta^2+V(x)\Psi_\alpha(x)=E\Psi_\alpha(x),$$

which we rewrite, replacing $\Psi_{\alpha\pm1}$ by Ψ_α by means of Eq. (46),

$$-\frac{d^2}{dx^2}\Psi_\alpha(x)+\hat{T}_{ch}\Psi_\alpha(x)+\tilde{V}(x)\Psi_\alpha(x)=E\Psi_\alpha(x), \quad (48)$$

where the new effective potential $\tilde{V}$ has the form

$$\tilde{V}(x)=V(x)+[\exp(-i\gamma)-2+\exp(i\gamma)]/\Delta^2. \quad (49)$$

Equation (48) admits separation of the variables x and α. As a result, we obtain two one-dimensional problems: one is a Sturm–Liouville equation on a finite interval of length R with homogeneous (but complex) boundary conditions (47), and the other is for the free motion with respect to the discrete variable α described by the second-order difference equation [$\Psi_{\alpha n\varepsilon}(x)=\Psi_n(x)\chi_{\alpha\varepsilon}$]

$$-\frac{d^2}{dx^2}\Psi_n(x)+\tilde{V}(x)\Psi_n(x)=\varepsilon_n\Psi_n(x); \quad (50)$$

$$\left.\begin{aligned}&\Psi_n(0)=\exp(i\gamma)\Psi_n(R);\ \Psi'_n(0)=\exp(i\gamma)\Psi'_n(R);\\ &-(\chi_{\alpha+1,\lambda}-2\chi_{\alpha\lambda}+\chi_{\alpha-1,\lambda})/\Delta^2=\lambda\chi_{\alpha\lambda},\ \lambda=1-\cos\gamma.\end{aligned}\right\} \quad (51)$$

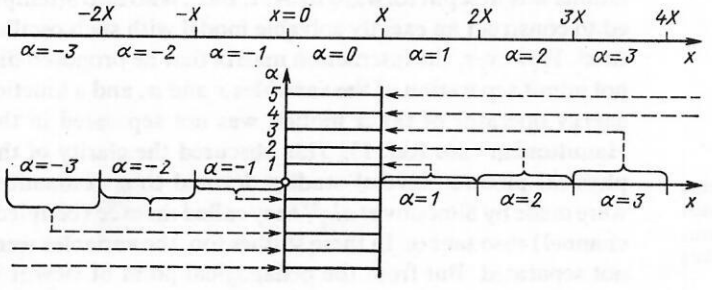

FIG. 25. "Rearrangement" of the x axis in Fig. 25a, divided into periods of α, into the two-dimensional (α,x) region in the form of an infinite ladder (b) of finite intervals (periods) labeled by the index α (see Fig. 25a). The two types of motion along x (standing waves within one period and free "motion through the periods") are more readily grasped when separated in the two-dimensional ladder (b).

The spectrum of the problem (50) with boundary conditions corresponding to (47) is purely discrete, while (45) is the difference analog of the Schrödinger equation for free motion. For such an equation there corresponds a continuous spectrum, but only on a bounded interval (allowed energy band), and as a result a band spectrum is obtained. Although the proposed method of treating the Bloch problem is equivalent in its physical essence to the usual description, it is pedagogically preferable to separate the two forms of motion along the single x axis—the oscillations within one period and the "motion with respect to the periods"—to avoid confusing them and to associate simpler equations with each of them.

To emphasize the commonality with other problems, it was suggested in Ref. 95 that the independent solutions in a periodic field should be called "Bloch sines, cosines, and exponentials with real and imaginary frequencies," in the same way that one can associate Bessel functions with sines, Neumann functions with cosines, and Hankel functions with exponentials, or one can speak of "Coulomb, quasipotential sines," etc. General solutions on arbitrary intervals are constructed from linear combinations determined from matching conditions. In paticular, one can "fit" into a periodic field a section in which a band of oscillatory solutions [allowed band] enters a forbidden energy band of the complete system, where the solutions grow or are damped exponentially. Thus, in a forbidden band one can obtain a bound state (even *above*) the continuum]. Conversely, a piece of a gap in a conduction band plays the part of an effective potential barrier. Combinations of such barriers can make systems with resonance tunneling for Bloch waves. Shifts of bands on finite intervals can be achieved by means of additional potentials, for example, potentials constant on a certain section of the axis ($\pm V_0 = \text{const}$ gives a parallel shift upward and downward, respectively). It is of interest to consider the time evolution of the tunneling of wave packets constructed from Bloch waves (by analogy with Ref. 91).

Bloch solutions can be used in the various approaches of the inverse problem (on the complete axis,[96] on a half-axis in accordance with the Gel'fand–Levitan or Marchenko methods, on a finite interval in the R-matrix theory, etc.) in order to construct various square-integrable perturbations of the periodic field. Thus, one can construct potential corrections of Bargmann type, including ones with bound states in the conduction bands and in the forbidden bands.[95] All these models extend the set of elements of our "quantum constructor."

These arguments can also be extended to multichannel and multiparticle systems.[95] A matrix (multichannel) periodic problem also has a band spectrum. If at some point there is a wave only in one of the channels, then one can expect that at the neighboring points waves also appear in the other channels as a result of perturbations by the periodic field. However, there are N (the number of channels) channel eigenstates for which the relative weights of the channel functions remain unchanged when the coordinate x is shifted by a period. It would be interesting to use the multichannel technique to investigate the motion of two (or more) coupled particles in a periodic field.

Potential that varies periodically with the time

We now turn to the nonstationary problem

$$i\frac{d}{dt}\Psi(x,\ t)=\left[-\frac{d^2}{dx^2}+V(x,\ t)\right]\Psi(x,\ t), \tag{52}$$

where V varies with the time periodically with period T:

$$V(x,\ t)=V(x,\ t+T). \tag{52'}$$

We consider a steady regime in which the wave function at different periods but at the same point differs only by a phase factor:

$$\Psi(x,\ t)=\exp(\pm i\gamma)\,\Psi(x,\ t\pm T). \tag{53}$$

We introduce a new variable α, which labels the periods, and consider the motion of waves in the three-dimensional space (x,t,α). This is a problem equivalent to the original problem (52)–(52'). Suppose that with respect to x the motion is restricted by infinite potential walls at the points $x = 0, R$, and with respect to t we impose a homogeneous boundary condition corresponding to (53):

$$\Psi_\alpha(x,\ t)=\exp(\pm i\gamma)\,\Psi_{\alpha+1}(x,\ t). \tag{54}$$

As in the previous section, we can separate the free motion with respect to the variable α from the oscillations within a period,

$$\Psi_\alpha(x,\ t)=\Psi(x,\ t)\,\chi_\alpha;\quad \frac{\chi_{\alpha+1}-\chi_\alpha}{\Delta}=\lambda\chi_\alpha, \tag{55}$$

where λ is the so-called quasienergy, and we can solve separately the eigenvalue problem in the rectangle $0 \leqslant x \leqslant R$, $0 \leqslant t \leqslant T$ (Fig. 26):

$$[-i\partial/\partial t-\partial^2/\partial x^2+V(x,\ t)+2(\cos\gamma-1)/\Delta^2]\,\Psi_n(x,\ t)$$
$$=\varepsilon_n\Psi_n(x,\ t);$$
$$E=\varepsilon_n+\lambda.$$

The quasienergy (for free motion with respect to the discrete variable), like the quasimomentum, has a finite band of allowed values.

Trapping of waves in the continuum

We now turn to the study of *bound states immersed in the continuum*. They represent a rather rare phenomenon in the quantum world. But they are very interesting both for understanding of one of the mechanisms of formation of resonances (especially narrow ones), which have a similar nature, and from the pedagogical point of view (as an illustration of unexpected manifestations of quantum laws that

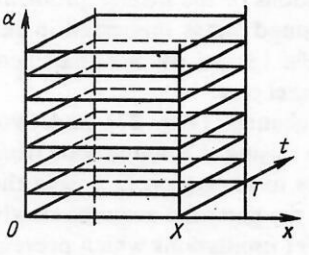

FIG. 26. Three-dimensional region in the (x,t,α) space. Free waves in the α direction together with standing waves of eigenstates on the rectangle $0 \leqslant x \leqslant X$, $0 \leqslant t \leqslant T$ in the (x,t) plane give the total wave function Ψ of the particle in an infinite one-dimensional rectangular well perturbed by an external periodic potential.

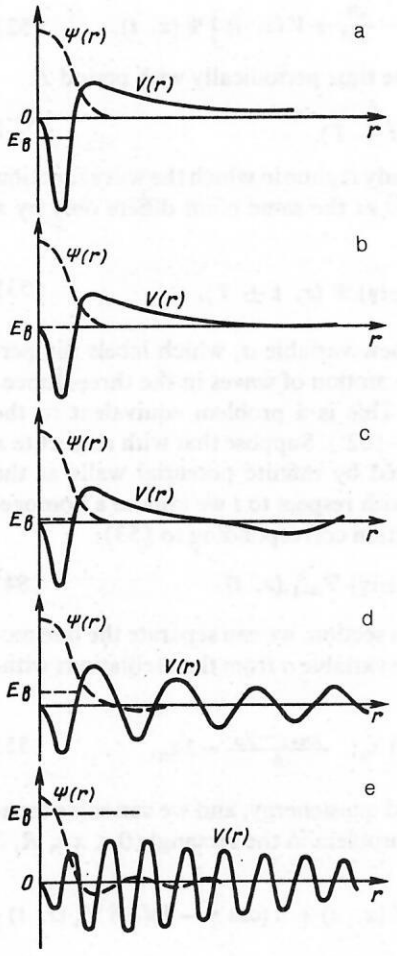

FIG. 27. Deformation of the potential when a state is raised from the region of negative energies to the continuum.[87]

permit a deeper understanding of the laws). The first examples of them in closed analytic form were already given by von Neumann and Wigner in 1929. Since then, bound states immersed in the continuum have attracted the attention of many physicsts and mathematicians. There has even been a monograph, by Eastham and Kalf[58] entirely devoted to such states [see also the book by Reed and Simon (Ref. 37, Vol. 3, Chap. 11, and Vol. 4, Chap. 13)]. In 1951, Gel'fand and Levitan[8] showed that one can readily construct potentials of Bargmann type that have bound states immersed in the continuum by means of the equations of the inverse problem. Several new single-channel bound states immersed in the continuum were found in Refs. 18 and 64. We shall here consider mainly the multichannel case.

We compare the single-channel (Fig. 27) and two-channel (Fig. 28) systems. On raising of a bound state from the region of negative energies to the region $E > 0$ in the single-channel case (Fig. 27) the potential acquires slowly damped [damped as $\sin(kr)/r$] oscillations which prevent the wave function from "flowing out."[87]

Channel coupling makes it possible to keep waves in the continuum as well by means of a short-range (exponentially decreasing; see Figs. 28b and 28c)[87] *interaction matrix*. This is possible if there is at least one closed channel (energy above the lower, $E_1 = 0$, but lower than the upper, $E_2 = 0$, threshold for opening of the channels). And it is only when the energy of the bound state is above the highest threshold (Figs. 28d and 28e) that weakly damped [as $\sin(kr)/r$] oscillations appear in the interaction matrix.

Figures 28f and 28g show the interaction matrices $V_{\alpha\beta}(r)$ corresponding to a bound state in the continuum at the same energy as in Fig. 28c but with changed normalization vector $\{c_1, c_2\}$ (the values of the derivatives of the channel functions Ψ_1 and Ψ_2 at the origin). For $c_1 = 1$, $c_2 = 0.1$, the influence of the closed channel is weakened [see Fig. 28f (cf. Fig. 28c, in which $c_1 = c_2 = 1$)]. In Fig. 28g, $c_1 = 1$, $c_2 = 2$. This is one further example of the part played by the normalization factors (the connection between variations of them and the form of the potential matrix).

We also mention here some simple examples of bound states in the continuum of this type: 1. Resonances above a rectangular barrier go over in the limit of infinite increase of the barrier height into bound states (Fig. 29). 2. Suppose that in a two-channel problem with different thresholds ε_1 and ε_2 [at $E = \varepsilon_\alpha$ the energy $E - \varepsilon_\alpha$ in channel α of the system (35) is equal to zero] at which the individual channels are opened the nondiagonal elements $V_{12}(x) = V_{21}(x)$ of the interaction matrix are made to tend to zero; then the bound states in the potential well $V_{22}(x)$ of the channel with the higher threshold that are situated between the threshold energies ε_1 and ε_2 become bound states in the continuum of the first open channel (Fig. 30).

COMMENTARIES ON THE LITERATURE

In its time, the inverse problem for the linear Schrödinger equation served to establish a new direction in physics and mathematics–the development of the effective *inverse-problem method* of solution of nonlinear equations (theory of solitons)—"one of the most beautiful discoveries of mathematical physics of the 20th century."[16] It has now become clear that most of the exactly solvable models known in "linear" quantum physics are unified from the point of view of the new mathematical formalism (see, for example, Refs. 10, 12, 24, and 50). New classes of exactly solvable models have appeared—it has been found that there exist analogs of the Bargmann potentials for nonstationary solutions of the Schrödinger equation [with two variables x and t (Refs. 10, 39, 59, and 66), and also in the multidimensional case[48]].

For example, the system of algebraic equations (24) of the stationary problem are generalized by the equations with time dependence [see Eq. (44) in Ref. 10]

$$\sum_{j=1}^{N}\left[C_{ij}+\frac{e^{i(\bar{\omega}_i-\omega_j)}}{\varkappa_i-\varkappa_j}\right]\Psi_j=-e^{i\bar{\omega}_i},\quad i=1,\ \ldots,\ N, \qquad (56)$$

where $\omega_i = \varkappa_i(x + \varkappa_i t)$, and the potential, which depends on the time, is determined by an expression like (29) [see Eq. (37) in Ref. 10]:

$$V(x,\ t) = 2\partial_x^2 \ln\det P(x,\ t),$$

where $P(x,t)$ is the matrix of coefficients in the system of equations (56). There is a similar close analogy between the expressions for the wave function at any energy in the stationary and nonstationary cases [cf. Eq. (4.3.19a) in Ref. 57

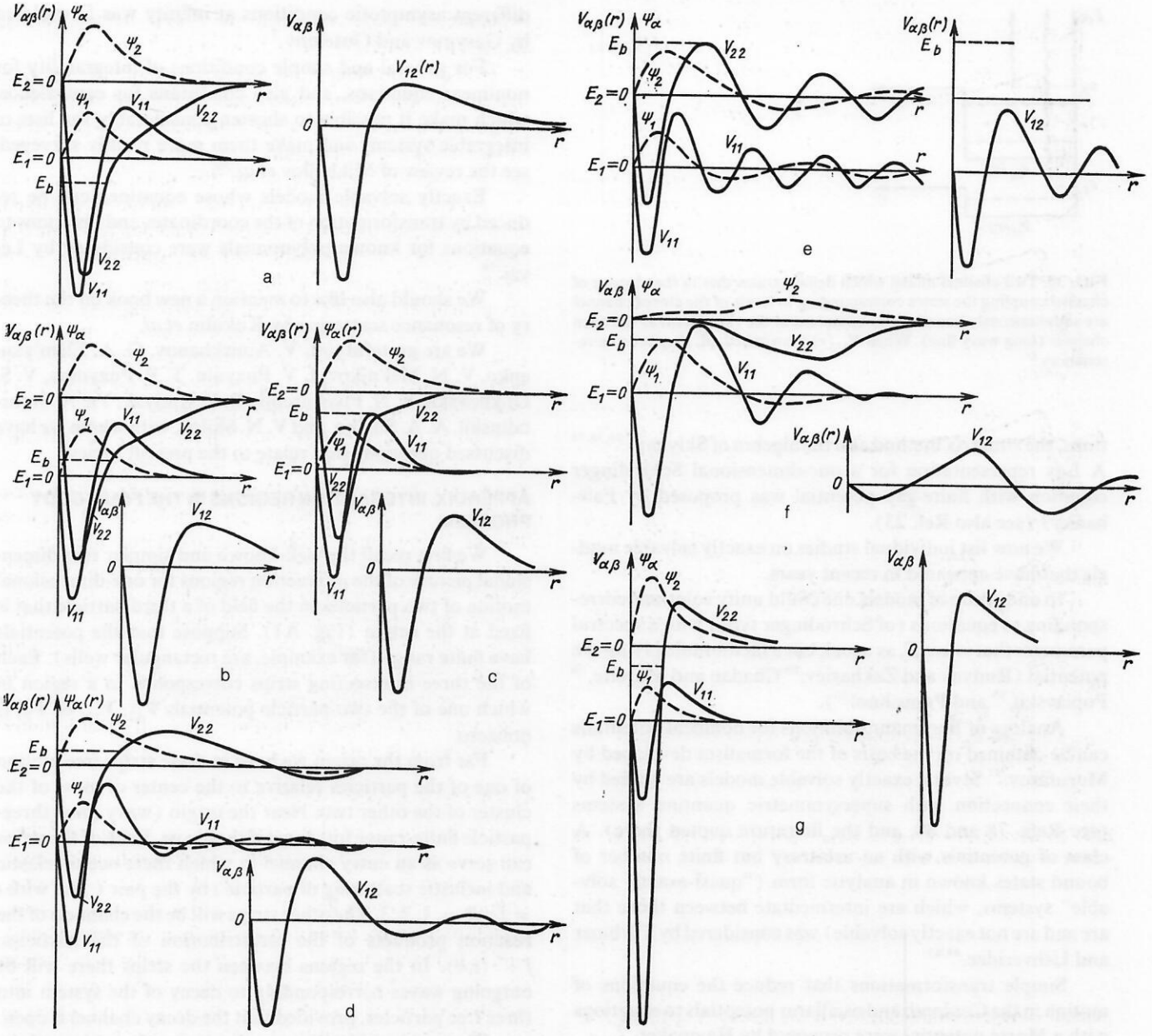

FIG. 28. Change of the interaction matrix $V_{\alpha\beta}(r)$ of a two-channel system wnen the level E_b of a bound state is raised. The channel wave functions Ψ_1 and Ψ_2 are shown by the broken curves: a) the level E_b is situated below the lowest threshold of the continuum (ordinary bound state); b) the energy E_b of the bound state is situated in the region of the continuum of the first channel (first channel open but the second closed); the interaction matrix with exponential decrease at large r completely prevents the wave from escaping from the interaction region; c) the same as in Fig. 28b, except that E_b is raised closer to the threshold of the continuum of the second channel, $E_2 = 0$; d) the bound state is in the region above the second threshold $E_2 = 0$; to confine the bound state it is now necessary to have oscillations of the tails of the elements V_{11}, V_{22}, $V_{12} = V_{21}$ of the potential matrix; e) the same as in Fig. 28d, except that the bound state is raised even higher, as a result of which the oscillations of $V_{\alpha\beta}$ are increased; f) the interaction matrix of a two-channel system with bound state in the continuum and with derivative at the origin of the function of the second channel 10 times smaller than in Fig. 28c; note the appearance of oscillations in V_{11}, although it remains a short-range potential; g) the same as in Fig. 28f with $c_1 = 1$, $c_2 = 2$.

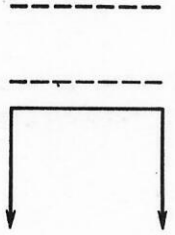

FIG. 29. Total above-barrier reflection from infinite potential steps leads to bound states situated above the top of the barrier; for infinite potential steps of barriers of finite height, these bound states become resonance states. The shape of the top of the barrier is not important for this.

and Eq. (36) in Ref. 10], despite the difference in the number of variables.

These nonstationary and multidimensional solutions have yet to be used to investigate the influence of variations of individual spectral parameters on the form of the corresponding fields in the manner of the "pictures" given in our review.

It is remarkable how intimate connections have been established between exact models from such seemingly widely separated fields as nonrelativistic quantum mechanics, field theory, and statistical physics.[5,16,42] Here, important parts have been played by the Lax and Yang–Baxter equa-

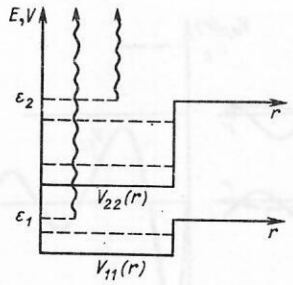

FIG. 30. Two-channel model which demonstrates that in the absence of channel coupling the states corresponding to levels of the closed channel are simultaneously bound states immersed in the continuum of the open channel (long wavy line). When $V_{12}(r)$ is switched off, they become resonances.[14]

tions, the r-matrix method and the algebra of Sklyanin [25,38,74] A Lax representation for a one-dimensional Schrödinger equation with finite-gap potential was proposed by Fairbanks[61] (see also Ref. 23).

We now list individual studies on exactly solvable models that have appeared in recent years.

In one group of models one could unify solutions corresponding to equations (of Schrödinger type) with a spectral parameter that is not E, as usual, but a factor multiplying the potential (Rudyak and Zakhariev,[85] Chadan and Musette,[56] Poplavskiĭ,[35] and Popushnoĭ[36]).

Analogs of Bargmann solutions for nonlocal potentials can be obtained on the basis of the formalism developed by Muzafarov.[31] Several exactly solvable models are unified by their connection with supersymmetric quantum systems (see Refs. 78 and 88, and the literature quoted there). A class of potentials with an arbitrary but finite number of bound states known in analytic form ("quasi-exactly solvable" systems, which are intermediate between those that are and are not exactly solvable) was considered by Turbiner and Ushveridze.[44,45]

Simple transformations that reduce the equations of motion in the Coulomb and oscillator potentials to equations with a Morse potential were proposed by Haymaker.[93]

The matrix generalization of the Krein–Crum–Darboux transformations for the case of different thresholds was considered by Humi[70] and Suz'ko[40] (for the multidimensional case, see Humi's paper[70]). L. M. Berkovich has told us that the transformations associated with the name of Darboux were already considered by Euler[60] in 1780–1794 and by Imshenetskiĭ[21] in 1882.

Noncentral Bargmann potentials that admit separation of the variables in spheroidal coordinates were considered by Funke and Zakhariev[64] and also by Suz'ko.[40]

Niznik,[32] considering the inverse problem for hyperbolic equations, gives examples of exactly solvable Dirac equations. A transformation that relates the Schrödinger, Klein–Gordon, and Dirac operators was proposed by Leon.[77]

The inverse scattering problem on a noncompact graph was considered by Gerasimenko,[9] and a new problem—the recovery of the potential from the positions of the nodes of the eigenfunctions—was considered in Ref. 68. For models with δ-function interactions, see Refs. 34 and 51.

A theorem on the two spectra for problems on a half-axis with common boundary condition at the origin and two different asymptotic conditions at infinity was formulated by Gasymov and Guseĭnov.[7]

For general and simple conditions of integrability for nonlinear equations, and also conditions for equivalence, which make it possible to shorten considerably the lists of integrable systems and make them more readily surveyed, see the review of Mikhaĭlov *et al.*[30]

Exactly solvable models whose equations can be reduced by transformation of the coordinates and functions to equations for known polynomials were considered by Lévai.[78]

We should also like to mention a new book on the theory of resonance scattering by Kukulin *et al.*[73]

We are grateful to I. V. Amirkhanov, G. A. Elem'yanenko, V. N. Mel'nikov, I. V. Puzynin, T. P. Puzynina, V. S. Ol'khovskiĭ, V. N. Pivovarchik, B. V. Rudyak, Ya. A. Smorodinskiĭ, A. A. Suz'ko, and V. N. Shilov, with whom we have discussed questions that relate to the present review.

APPENDIX. INTERACTION REGIONS IN THE FOUR-BODY PROBLEM

We first recall the well-known and simpler two-dimensional picture of the interaction regions for one-dimensional motion of two particles in the field of a third particle that is fixed at the origin (Fig. A1). Suppose that the potentials have finite range (for example, are rectangular wells). Each of the three intersecting strips corresponds to a region in which one of the two-particle potentials V_{12}, V_{13}, or V_{23} is nonzero.

Far from the origin we have in these strips free motion of one of the particles relative to the center of mass of the cluster of the other two. Near the origin (wavy line) three-particle finite-range forces act if they exist. Each of the strips can serve as an entry channel in which there occurs elastic and inelastic scattering of particle i by the pair (j,k) with $i \neq j \neq k = 1, 2, 3$. The other strips will be the channels of the reaction products of the redistribution of the particles: $j + (i,k)$. In the regions between the strips there will be outgoing waves corresponding to decay of the system into three free particles, provided that the decay channel is open.

We now consider the one-dimensional problem of the motion of three particles in the field of a force, which is situated at the point $x = 0$ (see Fig. A2a); the particles interact with one another by means of rectangular wells. In the center-of-mass system (in our case the center of mass is at the position of the fourth particle), the configuration space is already three-dimensional. The region in which the potential V_{ij} of the interaction of particles i and j is nonzero is

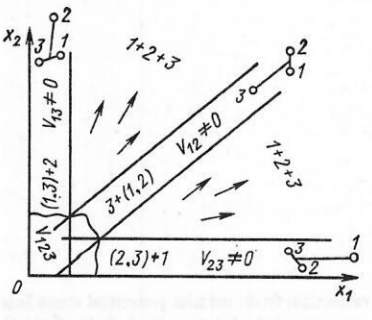

FIG. A1. System of three particles executing one-dimensional motion along an axis on which the third particle is fixed at the point $x = 0$.

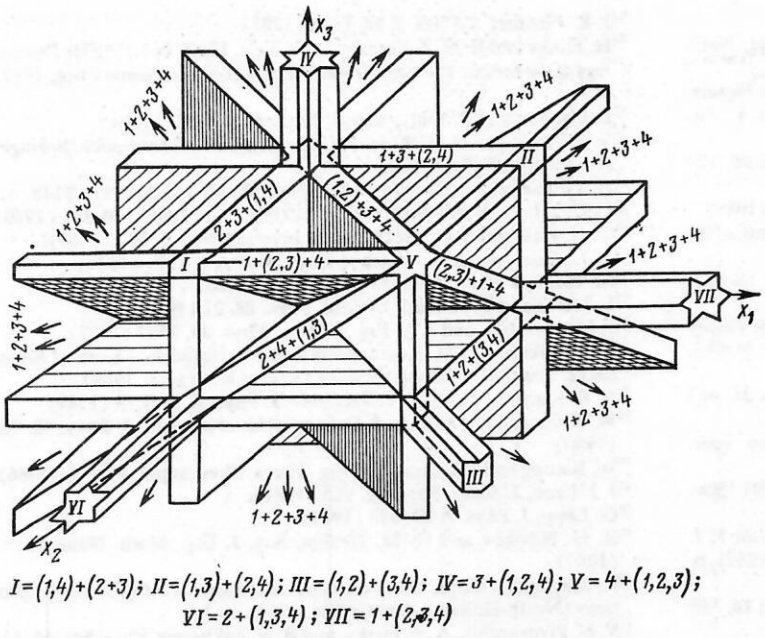

FIG. A2. Regions of interaction of particles 1, 2, 3 with particle 4, which is fixed at the origin of the three-dimensional configuration space of the four-particle system. The six flat layers corresponding to the regions in which the short-range potentials V_{12} $V_{13}, V_{14}, V_{23}, V_{24}, V_{34}$ are nonzero (for each two-particle potential there is a corresponding layer) intersect, passing at different angles through the origin. The seven cylindrical "tubes" (formed by the intersections of the layers) that emanate from the center (from the fourth particle) correspond to interaction of bound pairs of particles $(1,4)+(2,3)$, $(1,2)+(3,4)$, $(1,3)+(2,4)$ (three tubes with cross section in the form of rectangles) or of bound triplets of particles with the remaining particle (four tubes with cross section in the form of six-pointed stars; the shape of the cross sections depends on the ratios of the widths of the potentials). The regions outside the layers correspond to complete decay of the system: $1+2+3+4$.

a flat layer with thickness equal to the thickness of the potential well (within such a layer, these two particles are near each other, while the others can be situated arbitrarily, both with respect to each other and with respect to the given pair). The intersection of two mutually orthogonal layers is a "tube" in which the particles are grouped in two pairs of interacting particles, $(i,j)+(k,l)$, the distance between the pairs varying along the tube. In Fig. A2, three such tubes have a rectangular cross section. At an intersection of three layers there is formed a tube whose interior corresponds to a compact three-particle cluster (i,j,k) and a fourth particle, whose distance from the cluster varies along the tube (see the four tubes in Fig. A2 with section in the form of six-pointed stars). In such tubes, the three-particle interactions may also be nonzero. The short-range four-particle forces are nonzero near the origin.

[1)] In particular, knowledge of this rule enabled us to find more quickly bugs in a level-shift program written for a personal computer.

[2)] Potentials that have a shape symmetric with respect to their center are uniquely determined by the energy levels without specification of the normalization constants γ (see Ref. 20, p. 40), which adjust themselves to the given level spectrum.

[1]A. I. Baz', Zh. Eksp. Teor. Fiz. **70**, 397 (1976) [Sov. Phys. JETP **43**, 205 (1976)].

[2]L. M. Berkovich, *Transformation of Ordinary Linear Differential Equations* [in Russian] (Publishing House of Kuibyshev University, Kuibyshev, 1978).

[3]I. V. Bogdanov, Teor. Mat. Fiz. **65**, 35 (1985).

[4]I. V. Bogdanov and Yu. N. Demkov, Zh. Eksp. Teor. Fiz. **93**, 3 (1987); **82**, 1798 (1982) [Sov. Phys. JETP **66**, 1 (1987); **55**, 1037 (1982)].

[5]R. Baxter, *Exactly Solved Models in Statistical Mechanics* (Academic Press, New York, 1982) [Russ. transl., Mir, Moscow, 1985].

[6]A. A. Vladimirov, *Introduction to Quantum Integrable Systems Lectures for Young Scientists*), R17-85-742 [in Russian] (Dubna, 1985).

[7]M. G. Gasymov and G. Sh. Guseĭnov, Dif. Uravn. **25**, 588 (1989).

[8]I. M. Gel'fand and B. M. Levitan, Izv. Akad. Nauk SSSR, Ser. Mat. **15**, 309 (1951).

[9]N. I. Gerasimenko, Teor. Mat. Fiz. **75**, 187 (1988).

[10]B. A. Dubrovin, T. M. Malanyuk, I. M. Krichever, and V. G. Makhan'kov, Fiz. Elem. Chastits At. Yadra **19**, 579 (1988) [Sov. J. Part. Nucl. **19**, 252 (1988)].

[11]B. A. Dubrovin, V. B. Matveev, and S. P. Novikov, Usp. Mat. Nauk **31**, 55 (1976).

[12]B. A. Dubrovin, Usp. Mat. Nauk **36**, 11 (1981); Funkts. Anal. Prilozh. **9**, 41 (1975).

[13]V. P. Zhigunov and B. N. Zakhar'ev, *Methods of Strong Channel Coupling in Quantum Scattering Theory* [in Russian] (Atomizdat, Moscow, 1974).

[14]V. P. Zhigunov, B. N. Zakhar'ev, S. A. Niyazgulov, and A. A. Suz'ko, Preprint R4-7815 [in Russian], JINR, Dubna (1974).

[15]V. I. Zagrebaev, in *Elementary Processes in Collisions of Atomic and Molecular Particles* [in Russian] (Publishing House of Cheboksary State University, Cheboksary, 1977); Yad. Fiz. **49**, 1630 (1989) [Sov. J. Nucl. Phys. **49**, 1009 (1989)]; Ann. Phys. (N.Y.) **197**, 33 (1990).

[16]V. E. Zakharov, S. V. Manakov, S. P. Novikov, and L. N. Pitaevskiĭ, *The Theory of Solitons* [in Russian] (Nauka, Moscow, 1980).

[17]V. E. Zakharov and A. B. Shabat, Zh. Eksp. Teor. Fiz. **61**, 118 (1971) [Sov. Phys. JETP **34**, 62 (1971)].

[18]B. N. Zakhar'ev, V. N. Pivovarchuk, and A. A. Suz'ko, in *Theory of Quantum Systems with Strong Interaction* [in Russian] (Publishing House of Kalinin State University, Kalinin, 1985), p. 69.

[19]B. N. Zakhar'ev and E. B. Plekhanov, Preprint R4-89-287 [in Russian], JINR, Dubna (1989).

[20]B. N. Zakhar'ev and A. A. Suz'ko, *Potentials and Quantum Scattering. The Direct and Inverse Problems* [in Russian] (Énergoatomizdat, Moscow, 1985).

[21]V. G. Imshenetskiĭ, Zap. Imp. St.-Peterb. Mineral. Ob. **42**, 1 (1882).

[22]V. A. Kolkunov, Yad. Fiz. **10**, 1296 (1969) [Sov. J. Nucl. Phys. **10**, 734 (1970)].

[23]N. A. Kostov, Lett. Math. Phys. **17**, 95 (1989).

[24]I. M. Krichever, Usp. Mat. Nauk **44**, 121 (1989).

[25]V.B. Kuznetsov, "Application of the inverse scattering method in the theory of two-dimensional integrable classical and quantum dynamical systems," Candidate's Dissertation [in Russian] (Leningrad, 1989).

[26]Yu A. Kuperin, Teor. Mat. Fiz. **69**, 100 (1986); **75**, 431 (1988).

[27]B. M. Levitan, *Inverse Sturm–Liouville Problems* (VNU Science Press, Utrecht, 1987) [Russ. original, Nauka, Moscow, 1984].

[28]A. M. Lane and R. G. Thomas, Rev. Mod. Phys. **30**, 257 (1958) [Russ. transl., IL, Moscow, 1960].

[29]V. É. Lyantse, Mat. Sb. **72(114)**, 537 (1967).

[30]A. V. Mikhaĭlov, A. B. Shabat, and R. I. Yamilov, Usp. Mat. Nauk **42**, 3 (1987).

[31]V. M. Muzafarov, Teor. Mat. Fiz. **70**, 30 (1987); **64**, 208 (1985); Inverse Probl. **4**, 185 (1988); Mod. Phys. Lett. **2**, 177, 239 (1987); **1**, 449 (1986).

[32]L. P. Niznik, Rep. Math. Phys. **26**, 261 (1988).

[33]V. S. Ol'khovskiĭ, Fiz. Elem. Chastits At. Yadra **15**, 289 (1984) [Sov. J. Part. Nucl. **15**, 130 (1984)].

[34]B. S. Pavlov, Usp. Mat. Nauk **42**, 99 (1987).

[35]I. V. Poplavskiĭ, Izv. Akad. Nauk SSSR, Ser. Fiz. **51**, 97 (1987); Yad. Fiz. **44**, 952 (1986) [Sov. J. Nucl. Phys. **44**, 614 (1986)]; Teor. Mat.

Fiz. **69(3)**, 475 (1986).
[36]M. N. Popushoĭ, Teor. Mat. Fiz. **69**, 466 (1986); Izv. Akad. Nauk SSSR, Ser. Fiz. **52**, 150 (1988); **51**, 952 (1987).
[37]M. C. Reed and B. Simon, *Methods of Modern Mathematical Physics*, Vol. 4 (Academic Press, New York, 1978) [Russ. transl., Vol. 4, Mir, Moscow, 1982].
[38]E. K. Sklyanin, Zap. Nauchn. Semin. Leningr. Ot. Mat. Inst. **95**, 129 (1980).
[39]S. I. Slavov, Preprint R5-89-261 [in Russian], JINR, Dubna (1989).
[40]A. A. Suz'ko, Phys. Scr. **31**, 447 (1985); **34**, 5 (1986); *Proceedings of the Few Body Conf. 11* (Japan, 1986); Sov. Eng. Phys. J. **50**, 316.
[41]A. V. Tarakanov and V. M. Shilov, Yad. Fiz. **48**, 109 (1988) [Sov. J. Nucl. Phys. **48**, 68 (1988)].
[42]L. A. Takhtajan and L. D. Faddeev, *Hamiltonian Methods in the Theory of Solitons* (Springer-Verlag, Berlin, 1987) [Russ. original, Nauka, Moscow, 1986].
[43]N. F. Truskova, Yad. Fiz. **36**, 790 (1982) [Sov. J. Nucl. Phys. **36**, 463 (1982)].
[44]R. T. Turbiner, Funkts. Anal. Prilozh. **22**, 92 (1988); Zh. Eksp. Teor. Fiz. **94**, 33 (1988) [Sov. Phys. JETP **67**, 230 (1988)].
[45]A. G. Ushveridze, Fiz. Elem. Chastits At. Yadra **20**, 1185 (1989) [Sov. J. Part. Nucl. **20**, 504 (1989)].
[46]L. D. Faddeev, in *Jubilee Collection of the Leningrad Branch of the V. I. Steklov Mathematics Institute* [in Russian] (Nauka, Moscow, 1987), p. 4.
[47]G. F. Filippov, Fiz. Elem. Chastits At. Yadra **15**, 1338 (1984); **16**, 349 (1985) [Sov. J. Part. Nucl. **15**, 600 (1984); **16**, 153 (1985)].
[48]V. I. Fushchich, V. M. Shtelen', and N. I. Serov, *Symmetry Analysis and Exact Solutions of Nonlinear Equations of Mathematical Physics* [in Russian] (Naukova Dumka, Kiev, 1989).
[49]E. Kh. Khristov, "Nonlinear evolution equations for approximate solution of inverse problems of spectral analysis," Doctoral Dissertation [in Russian] (Dubna, 1981).
[50]I. V. Cherednik, Funkts. Anal. Prilozh. **12**, 45 (1978).
[51]S. Albeverio, P. Gestezy, R. Hoegh-Kron, *et al.*, in *Solvable Models in Quantum Mechanics* (Springer, Heidelberg, 1988).
[52]I. V. Amirkhanov, I. V. Puzynin, T. P. Puzynin, *et al.*, in *Proceedings of the Conf. on Schrödinger Operators, Standard and Nonstandard, Dubna, 1988* (World Scientific, Singapore, 1989), p. 353; Preprint E4-89-312, JINR, Dubna (1989).
[53]A. M. Badalyan, L. P. Kok, M. I. Polikarpov, and Yu. A. Simonov, *Resonances in Coupled Channels in Nuclear and Particle Physics* (University of Groningen, 1981).
[54]S. Brand and H. D. Dahmen, *The Picture Book of Quantum Mechanics* (Wiley, New York, 1985).
[55]K. Chadan and A. Montes, J. Math. Phys. **9**, 1898 (1968).
[56]K. Chadan and M. Musette, Inverse Probl. **5**, 257 (1989); C. R. Acad. Sci. (Paris) **305**, 1409 (1987); **303**, 329 (1987); **299**, 1305 (1987).
[57]K. Chadan and P. Sabatier, *Inverse Problems in Quantum Scattering Theory* (Springer, Heidelberg, 1977).
[58]M. S. P. Eastham and H. Kalf, *Schrödinger-Type Operations with Continuous Spectra* (Pitman, London, 1982).
[59]V.-Z. Enolskii and N. A. Kostov, Preprint, Lab. Appl. Phys. Techn. Univ., Denmark (1989).
[60]L. Euler, Acad. Exhib. 13, Jan. (1780); Institutiones Calculi Integralis **4**, 533 (1794).
[61]L. D. Fairbanks, Compositio Math. **68**, 31 (1988).
[62]D. J. Fernandez, Lett. Math. Phys. **8**, 337 (1984).
[63]J. R. Fletcher, J. Phys. C **18**, L-55 (1985).
[64]H. Funke and B. N. Zakhariev, Phys. Lett. **185B**, 265 (1987); *Proceedings of the Inverse Problems, 1986, Montpellier* (Academic Press, 1987), p. 99.
[65]L. Gagnon and P. Winternitz, J. Phys. A **22**, 469 (1989).
[66]V. P. Gerdt and N. A. Kostov, *Computers and Mathematics* (Springer, Heidelberg, 1989), p. 279.
[67]H. Grosse and A. Martin, Nucl. Phys. **B132**, 125 (1978); **B148**, 413 (1979); Lect. Notes Phys. **116**, 68 (1979); Phys. Rep. C **60**, 341 (1980).
[68]O. H. Hald and J. R. McLaughlin, Inverse Probl. **5**, 307 (1989).
[69]E. J. Heller and H. A. Yamani, Phys. Rev. A **9**, 1201 (1974).
[70]M. Humi, J. Phys. A **21**, 2075 (1988); **18**, 1085 (1985).
[71]L. Infeld and T. E. Hull, J. Math. Phys. **23**, 21 (1951).
[72]J. M. Kovalsky and J. L. Fry, J. Math. Phys. **28**, 2407 (1987).
[73]V. I. Kukulin, V. M. Krasnopolsky, and J. Horáček, *Theory of Resonances. Principles and Applications* (Scademia, Prague, 1989).
[74]V. B. Kuznetsov and A. V. Tsiganov, J. Phys. A **22**, L73 (1989).
[75]W. Kwong, J. L. Rosner, J. F. Schonfeld, *et al.*, Am. J. Phys. **48**, 926 (1980).
[76]W. Kwong and J. L. Rosner, Prog. Theor. Phys. Suppl. **86**, 366 (1986).
[77]J. J. Leon, J. Math. Phys. **22**, 965 (1981).
[78]G. Lévai, J. Phys. A **22**, 689 (1989).
[79]R. G. Novikov and G. M. Henkin, Sov. J. Usp. Math. Nauk **42**, 93 (1987).
[80]R. May and J. Noye, *Computational Techniques for Differential Equations* (North-Holland, Amsterdam, 1984), p. 1.
[81]V. N. Pivovarchik, A. A. Suzko, and B. N. Zakhariev, Phys. Scr. **34**, 101 (1986).
[82]E. B. Plekhanov, A. A. Suzko, and B. N. Zakhariev, Ann. Phys. (Leipzig) **39**, 313 (1982).
[83]J. Poschel and E. Trubowitz, *Inverse Spectral Theory* (Academic Press, Boston, 1987).
[84]I. Rotter, Fiz. Elem. Chastits At. Yadra **19**, 274 (1988) [Sov. J. Part. Nucl. **19**, 118 (1988)]; I. Rotter and Kleinwachter, Phys. Rev. C **32**, 1742 (1985).
[85]B. V. Rudyak and B. N. Zakhariev, Inverse Probl. **3**, 125 (1987).
[86]J. F. Schonfeld, W. Kwong, J. Rosner, *et al.*, Ann. Phys. (N.Y.) **128**, 1 (1980).
[87]F. H. Stillinger and D. R. Herrik, Phys. Rev. A **11**, 446 (1975).
[88]C. V. Sukumar, J. Phys. A **18**, 2917 (1985).
[89]H. B. Thaker, C. Quigg, and J. L. Rosner, Phys. Rev. D **21**, 234 (1980).
[90]B. N. Zakhariev, *Few-Body Systems*, Vol. 4 (1988), p. 25; *Inverse Problems* (Academic Press, 1987), p. 141; *Order, Disorder and Chaos in Quantum Systems* (World Scientific, Singapore, 1989), p. 171.
[91]B. N. Zakhariev, V. S. Olkhovsky, and V. M. Shilov, Preprint R4-89-289 [in Russian], JINR, Dubna (1989).
[92]B. N. Zakhariev and L. G. Zastavenko, Phys. Rev. A **39**, 5528 (1989); Preprint R4-88-662 [in Russian], JINR, Dubna (1988).
[93]R. H. Haymaker and A. R. P. Rau, Am. J. Phys. **54**, 928 (1989).
[94]V. M. Dubovik, B. L. Markovsky, A. A. Suzko, *et al.*, Phys. Lett. **185B**, 1371 (1989); S. I. Vinitskiĭ, M. V. Kadomtsev, A. A. Suz'ko, Yad. Fiz. **48**, 1325 (1988) [Sov. J. Nucl. Phys. **48**, 841 (1988)].
[95]B. N. Zakhar'ev, Preprint R4-90-46 [in Russian], JINR, Dubna (1990).
[96]N. E. Firsova, Zap. Nauchn. Semin. Leningr. Ot. Mat. Inst. **51**, 183 (1975).

Translated by Julian B. Barbour